Sustainability analysis for the design of distributed energy systems: A multi-objective optimization approach

Juan Fonseca, Jean-Marc Commenge, Mauricio Camargo, Laurent Falk, Iván Gil

Sustainability Analysis for the Design of Distributed Energy Systems: A Multi-objective Optimization Approach

Juan D. Fonseca [a,c*], Jean-Marc Commenge [b], Mauricio Camargo [a], Laurent Falk [b], Iván D. Gil [c]

[a] Équipe de Recherche sur les Processus Innovatifs (ERPI), Université de Lorraine, 8 rue Bastien Lepage, 54000 Nancy Cedex, France

[b] Laboratoire Réactions et Génie des Procédés (LRGP), Université de Lorraine, 1 rue Grandville, BP 20451, 54001 Nancy Cedex, France

[c] Grupo de Procesos Químicos y Bioquímicos, Department of Chemical and Environmental Engineering, Universidad Nacional de Colombia – Sede Bogotá, Carrera 30 45-03, Bogotá, Colombia

Corresponding author: jdfonsecag@unal.edu.co

Abstract

The design of sustainable energy systems requires to enlarge the analysis beyond the traditional boundaries for including the economic, environmental, and societal needs and constraints in the decision-making process. In this regard, this work investigates the conceptual design of distributed energy systems by means of a multi-objective optimization strategy to simultaneously address the economic, environmental, and social aspects in the energy system design. Initially, the water consumption and the inherent safety indicators were introduced and evaluated through two single-objective optimization problems to enhance the analysis of the environmental and social dimensions of sustainability. Then, a framework including the total annualized cost, CO_2 emissions, water consumption, grid dependence, and inherent safety index was used to perform the multi-objective analysis. To carry out a thorough and comprehensive analysis, four optimization problems including different combinations of the sustainability indicators were proposed and solved. The compromise among the objective functions was identified, and the obtained Pareto sets were explored for elucidating the changes in the design and operating conditions across the non-dominated solutions. According to results, the cost of energy can range between 0.37 and 0.63 €/kWh, the CO_2 emissions can vary between 10.6 and 68.5 $kgCO_2/MWh$, and the water consumption can be between 27.8 and 70.2 m^3H_2O/GWh depending on the evaluated objective. Moreover, it was determined that the safety of the energy system can be improved by increasing the use of the water electrolysis pathway to produce hydrogen and by reducing the capacity of the hydrogen storage unit.

Keywords

Renewable energy, hybrid energy system, inherent safety index, hydrogen, sustainability assessment, decision-making.

Nomenclature

$H_{2,El}^{m}$	Mass flow rate of hydrogen from electrolyzer (kg/s)	I_{TOX}	Toxicity score
LHV_{H2}	Low heating value of hydrogen (kJ/kg)	I_{COR}	Corrosiveness score
H_2O_R	Mass flow rate of water to the reformer (kg/s)	I_R	Reaction score
AD_{in}	Input biomass to the anaerobic digester (kg/s)	I_I	Inventory score
H_2O_{FC}	Mass flow rate of water from the fuel cell (kg/s)	I_T	Temperature score
WC	Water consumption of the energy system (kgH_2O/year)	I_{Pr}	Pressure index
R_{out}	Output power of the reformer (kW)	k	Technology index
FC_{in}	Input power to the fuel cell (kW)	J	Performance criterion
MW_{H2}	Molecular weight of hydrogen (kg/kmol)	u	Decision variables
MW_{H2O}	Molecular weight of water (kg/kmol)	t	Time
I_C	Chemical safety index	S_{H2}	Energy stored in hydrogen form (kWh)
I_P	Process safety index	Bio_D	Biomass available for digestion (kg/year)
I_{FL}	Flammability score	S_B	Energy stored in the battery (kWh)
I_{EX}	Explosiveness score		

Greek letters

φ	Source of electricity for demand
θ	Source of hydrogen
α	Source of electricity for electrolysis
δ	Electricity storage option
γ	Source of methane for reforming
ψ_{El}	Water consumption in electrolysis (kgH_2O/kgH_2)
ψ_{AD}	Water consumption in anaerobic digestion (kgH_2O/kg biomass)

Abbreviations

DES	Distributed energy systems
HAZOP	Hazard and operability
P&ID	Piping and instrumentation diagram
PIIS	Prototype index of inherent safety
ISI	Inherent safety index
EISI	Enhanced inherent safety index
CISI	Comprehensive inherent safety index

1. Introduction

The current situation due to the coronavirus pandemic (Covid-19) has represented great impacts on global health, economy, energy use and CO_2 emissions. Indeed, because of these unprecedent circumstances, the economic curtailment has led to a decline in energy demand of 3.8% with respect to the first quarter of 2019. In this respect, according to the perspectives of the International Energy Agency, the annual energy demand will decrease between 4 and 6%. In the same line, it is expected the CO_2 emissions push down by 8% relative to the 2019 [1].

Nevertheless, before the exceptional circumstances linked to this sanitary crisis, global energy demand grew by 2,3%, and CO_2 emissions had increased by 1.7% in 2018 [2]. This was mainly driven by the constant expansion of world economy and population, and the growing demand for heating and cooling in some parts of the world. Indeed, in 2018 around 20% of the increase in energy consumption was the consequence of some extreme weather conditions (cold and hot snaps) [2]. This situation represents a significant concern for the energy sector, since the raising

emissions trends of the last few years are not aligned with the Paris agreement for keeping the global temperature rise below 2°C [3]. Consequently, as a response to this scenario, a global energy transformation is underway to satisfy the continuous increase in the energy consumption and to meet the world environmental goals. This necessary change lies upon three main pillars: (i) to increase the share of renewable resources, (ii) to rise the usage of low-carbon electricity as end-use energy form, and (iii) to deploy the distributed generation of energy [3–5].

Furthermore, there is also a need to develop a global industry in a sustainable way [6,7], so that activities of the present do not compromise the ability of future generations to meet their own needs [8,9]. Broadly, sustainable development promotes the balance of three aspects: economic success, social acceptance, and environmental protection [8]. Taking this into account, it is noted that sustainability requires a holistic approach, and to enlarge the analysis out of the traditional system boundaries by including the economic, environmental and societal needs and constraints in the decision-making process [10,11]. Therefore, the sustainable design of energy systems requires to simultaneously integrate multiple and often contradictory criteria, i.e. to address a multi-objective optimization problem.

Considering the aforementioned aspects, sustainable energy systems should have four main characteristics: cost-efficiency, reliability, safety, and environmental-friendliness [12,13]. In principle, distributed energy systems (DES) seem to be a suitable alternative to the before mentioned challenges, since they fit well with the features of sustainable energy systems. DES rely on the energy consumption close to the generation site, so that energy efficiency is increased as the energy losses across long-distance transmission lines are avoided [12]. Distributed generation also promotes the use of local and renewable resources, thus it enhances self-sufficiency and energy security, and it offers an alternative to provide energy with low-carbon emissions [12,14].

1.1. Literature Review

A diverse range of research has been published addressing the design of DES by using multi-objective optimization approaches. Broadly, these works differ in the method used to solve the optimization problem and in the objective functions evaluated. For instance, Gabrielli et al. performed the analysis including the total annualized cost and the annual CO_2 emissions by means of the epsilon-constraint method. In fact, they carried out the energy system design under both, deterministic [15] and uncertain [16] scenarios for considering the unpredictable behavior of the weather conditions and energy demands. Jing et al. used the same method and objective functions, but they include benefit allocation constraints inspired from cooperative Game Theory [17]. Falke et al. proposed to decompose the optimization problem into three stages to

reduce the mathematical complexity, and they included the life cycle assessment to evaluate the emissions of CO_2 equivalents [18]. Ren et al. also evaluated the annual cost and CO_2 emissions as objective functions, but they focused upon the operation of the energy system and employed the compromise method to solve the multi-objective optimization problem [19]. Meanwhile, other works have employed the weighted sum method for transforming the problem into a single-optimization case. Di Somma et al. used this approach for the design of energy systems by evaluating the total cost and the exergy efficiency as criteria [20]. Dorotić et al. also used that method to address optimization problems including cost, CO_2 emissions, and exergy destruction as the objective functions [21,22]. In another study, Dufo-López and Bernal-Agustín employed a multi-objective evolutionary and genetic algorithms for the design of energy system considering the net present cost, the CO_2 emissions and the unmet load as obective functions [23].

Alvarado et al. proposed an optimization model for the selection and operation of technologies by incorporating real-time energy pricing and demands, fuel flexibility, and projections for various parameters [24]. Moreover, they considered the total cost and CO_2 emissions as objective functions and used the weighted sum method to solve the multi-objective optimization. Mayer et al. provided a design framework for hybrid energy systems [25]. Besides, they used a genetic algorithm to solve single and multi-objective optimization problems considering the net present cost and the environmental footprint (life cycle assessment) as objectives. Hou et al. adressed the multi-objective optimization of DES by considering three different operational strategies namely (i) heat load following, (ii) electrical load following, and (iii) load characteristic matching following [26]. They employed the epsilon-constraint method to analyze the minimization of the total cost and CO_2 emissions. Likewise, Karmellos and Mavrotas used the same approach and objective functions, but they focused on comparing two methodologies for the design of DES. The former to simultaneously size the available technologies, and the latter to select technologies with a predefined size [27]. Recently, Yan et al. used an approach based on multidisciplinary design optimization (MDO) to determine the best combination of technologies for different scenarios (building types and climate zones) in terms of economic and environmental impact [28].

Table 1 presents a summary of the literature review drawing the objectives, criteria and the approaches used by researchers for the design of DES. As depicted, the analysis is focused on economic and environmental criteria by evaluating objective functions such as the total cost and the CO_2 emissions. Moreover, in most cases the optimization approach is based on transforming the original problem into a single-objective one by using the weighting and epsilon-constraint methods. These methods are simple and effective for solving problems with few objectives.

Nevertheless, to build an evenly distributed set of non-dominated solutions, the optimization problem must be solved many times since a single point is obtained at a time.

Table 1. Objective function, criteria and optimization approach commonly used for the design of distributed energy systems. (Ec) economic, (Env) environmental, (Tec) technical criteria.

Authors	Objective Function	Criteria	Optimization Approach	Reference
Gabrielli et al.	Total cost – CO_2 emissions	Ec – Env	Epsilon-constraint	[15]
Jing et al.	Total cost – CO_2 emissions	Ec – Env	Epsilon-constraint	[17]
Falke et al.	Total cost - CO_2 equivalents	Ec – Env	NSGA-II	[18]
Ren et al.	Total cost – CO_2 emissions	Ec – Env	Compromise method	[19]
Di Somma et al.	Total cost – exergy efficiency	Ec – Tec	Weighted sum method	[20]
Dorotić et al.	Cost – CO_2 emissions - exergy	Ec – Env - Tec	Weighted sum method	[21,22]
Dufo-López et al.	Cost – CO_2 emissions – unmet load	Ec – Env - Tec	Evolutionary algorithm (multi-objective)	[23]
Alvarado et al.	Cost – CO_2 emissions	Ec – Env	Weighted sum method	[24]
Mayer et al.	Cost – CO_2 emissions (LCA)	Ec – Env	NSGA-II	[25]
Hou et al.	Cost – CO_2 emissions	Ec – Env	Epsilon-constraint	[26]
Karmellos et al.	Cost – CO_2 emissions	Ec – Env	Epsilon-constraint	[27]
Yan et al.	Life cycle cost - LCA	Ec – Env	Multidisciplinary design optimization (MDO)	[28]

1.2. Novelty of this Paper

As noted from the previous literature review, the design of energy systems is predominantly performed based upon economic and environmental criteria. Indeed, the multi-objective analysis has been focused on two main issues: cost and CO_2 emissions. In such a way, the obtained results leave aside the impact of additional indicators, and especially the influence of the social aspects on the design of energy systems. Thus, to address this issue, it is necessary to develop methodological tools that enable to analyze these socio-technical systems within the framework of sustainable development, i.e. considering their economic, environmental, and social aspects [29–31].

On the one hand, billions of people worldwide still currently lack of water for drinking and hygiene purposes [32]. Besides, water shortages due to climate change effects, make the use of water another factor of supreme importance for assessing industrial activities [33]. In fact, high water consumptions in energy conversion processes should be avoided since they are not sustainable [33–37]. Accordingly, water consumption appears as a suitable indicator for

evaluating the performance of the energy system and for enhancing the analysis of the environmental dimension of sustainability.

On the other hand, even though the energy system design is primarily a technical challenge, social aspects can become the most important factors for its successful implementation in the community [29]. In general, the social dimension is associated to the impacts on the quality of life, which lies on two main features: equity and health. Social equity involves the level of fairness and inclusiveness for energy resources distribution [38]. Indeed, this issue is included in one of the sustainable development goals proposed by United Nations (Goal 7), which consists in ensuring access to affordable, reliable, sustainable and modern energy for all [39]. Otherwise, the health aspect refers to the potential pollution, accidents, injuries, or fatalities derived from energy generation. In this respect, the pollution issue commonly falls into environmental dimension, as it is quantified with variables such as gas emissions, particulate matter, or contamination of water. Meanwhile, occupational accidents and public hazards are related with the inherent risk derived from the operation of conversion technologies (e.g. temperature and pressure conditions), and the properties of chemical compounds (e.g. flammability, toxicity) employed within energy systems [35–38,40,41]. In this line, inherent safety analysis is recognized as a proper indicator for evaluating the potential impacts on the health during the energy system design, since the selection of conversion technologies and process conditions could be rated according to their intrinsic properties [42,43].

Considering the foregoing, this work aims to perform a sustainability analysis for the design of energy systems. In such a way, the contribution of this study is twofold: (i) two new indicators, namely water consumption and inherent safety index, are introduced as objective functions to perform the design of energy systems; and (ii) the trade-offs among a set of sustainability indicators are investigated through a multi-objective optimization approach to obtain some general insights for the conceptual design of DES. Accordingly, the remainder of this document is structured as follows. First, two single-objective optimization problems focused on the water consumption and inherent safety indicators are addressed for studying the impact of the objective function on the design and operating conditions of the energy system. Then, these two indicators are added to the framework developed by Fonseca et al. [44], wherein the total annualized cost, the CO_2 emissions and the grid dependence were used as the indicators for the energy system design. Considering that the results of a multi-objective optimization problem with five objectives would be hard to analyze, the sustainability analysis is decomposed into four multi-objective optimization problems. These optimization cases include different combinations of the five sustainability indicators by simultaneously addressing three objectives at most. This strategy enables to obtain a thorough understanding about the relationships among the

objective functions since the results can be analyzed based on a three-dimension plot. Thereafter, the set of Pareto solutions is explored and analyzed for identifying the changes in the design and operating conditions across the optimization results. Finally, the main findings are summarized and conclusions are drawn.

2. Methodology

2.1. Energy System Description

The energy system being considered is depicted in Figure 1, which corresponds to that one previously studied by Fonseca et al. [44]. As observed, the energy sources include solar and biomass resources, in addition with the possibility of importing electricity and natural gas from the main grid. These energy inputs are converted and/or managed within the system to satisfy electricity and hydrogen demand. For tackling the mismatch between the energy availability from renewables and the demand, the surplus electricity is stored either in an electrical battery or in hydrogen form by using the power-to-power pathway (electrolyzer - pressurized tank - fuel cell). Meanwhile, hydrogen is obtained by means of water electrolysis or steam methane reforming processes. In the latter, the reforming reactor can be fed either by natural gas from the network or by biomethane from the biomass digestion process.

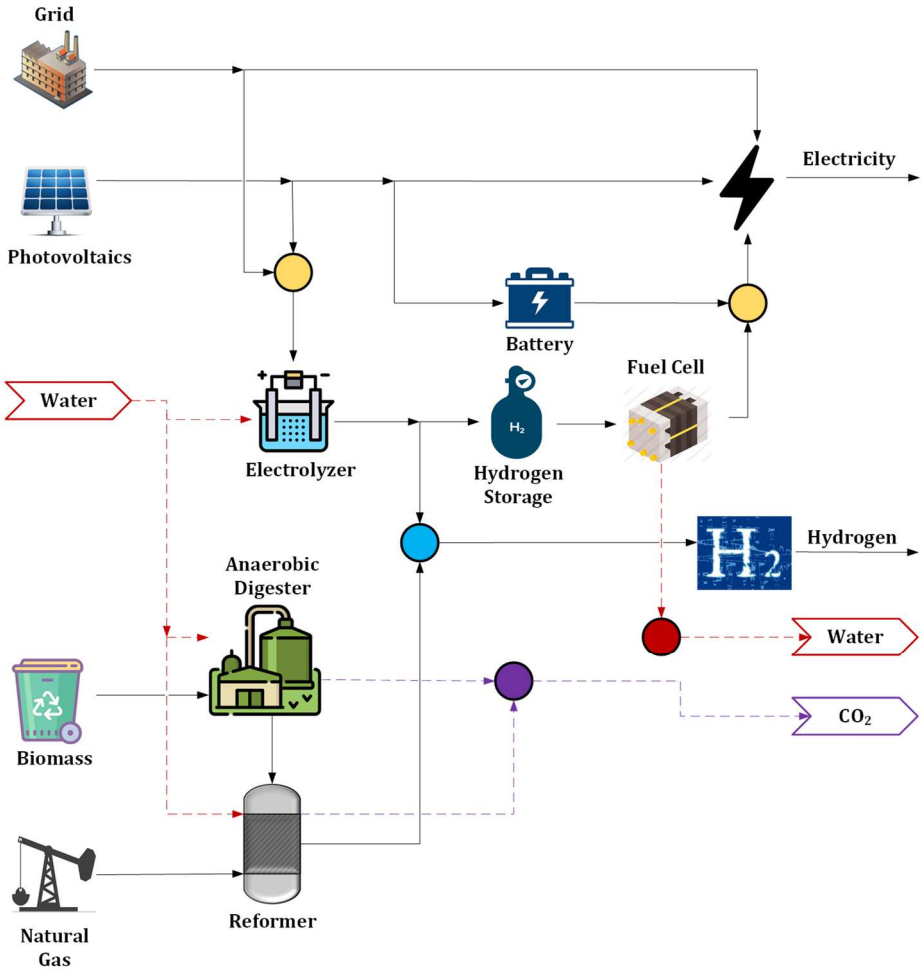

Figure 1. Schematic representation of the analyzed energy system. (●) electricity, (●) hydrogen, (●) water, (●) CO_2.

2.2. System Modeling and Case Study

The mass and energy balances, as well as the performance of the energy conversion and storage units are described according to the energy system model presented in reference [44]. Broadly, the system model has four main features:

1. It is a pseudo-steady state model, so that the time-dependence is taken into consideration but process units with instantaneous responses are assumed. Hence, accumulation within the energy converters is neglected. Moreover, the evolution of the energy stored is addressed by discretization of the temporal variable.
2. The operational conditions of energy converters are fixed; thus the input/output variables are related by means of constant efficiencies and linear expressions.
3. There are no energy losses across the connection lines.
4. The model is deterministic, and all the sizes of equipment are considered as continuous variables.

Moreover, the case study is a hypothetical neighborhood of 1500 inhabitants located at Marseille-France. The yearly electricity and hydrogen demands are 4080.6 and 731.5 MWh, respectively. Further details about the profiles of weather conditions (solar irradiance and ambient temperature), and energy demands can be found in [44]. Also, the corresponding set of performance and cost parameters is presented in that reference.

2.3. Single-objective Optimization

As mentioned in the introduction of this paper (Section 1), one of the contributions of this research lies on enhancing the sustainability evaluation of the energy system by including two new performance criteria. Therefore, the first step consisted in performing these single-objective optimizations. In the next sections, the objective functions and the formulation of the optimization problem are described.

2.3.1. Objective Functions

The optimization objectives proposed in this work are the annual water consumption and the inherent safety index. Accordingly, their corresponding mathematical formulation is presented as follows.

- *Water Consumption:*

According to the energy system structure (Figure 1), water is consumed in three operations: electrolysis (Equation 1), steam methane reforming (Equation 2), and anaerobic digestion. In the latter, water is mixed with the biomass for obtaining the slurry that is fed to the digester. Nevertheless, water is also obtained from the operation of fuel cell. In fact, this water is commonly recycled and reused in the electrolyzer.

$$2H_2O \rightarrow 2H_2 + O_2 \tag{1}$$

$$CH_4 + 2H_2O \leftrightarrow 4H_2 + CO_2 \tag{2}$$

Thus, the net water consumption (WC) of the energy system can be described by means of Equation 3. It is worthy to note that from the stoichiometry of water electrolysis reaction (Equation 1), 9kg of water are needed to produce 1kg of hydrogen. However, in practice around 11 kgH_2O/kgH_2 are required [45], which is represented by the factor ψ_{El}. Moreover, Equations 4 and 5 represent the water required in the reforming reactor and the water produced from fuel cell, respectively.

$$WC = \psi_{El} \int_{t0}^{tf} H_{2,El}^{m} dt + \int_{t0}^{tf} H_2O_R dt + \psi_{AD} \int_{t0}^{tf} AD_{in} dt - \int_{t0}^{tf} H_2O_{FC} dt \tag{3}$$

$$H_2O_R(t) = \left(\frac{R_{out}(t)}{LHV_{H2}}\right)\left(\frac{2MW_{H2O}}{4MW_{H2}}\right) \quad (4)$$

$$H_2O_{FC}(t) = \left(\frac{FC_{in}(t)}{LHV_{H2}}\right)\left(\frac{MW_{H2O}}{MW_{H2}}\right) \quad (5)$$

In these expressions, $H_{2,El}^{m}$ represents the amount of hydrogen produced by water electrolysis, H_2O_R the water required by reforming process, ψ_{AD} the water consumption of the anaerobic digestion process, and AD_{in} the input biomass to the digester. Moreover, H_2O_{FC} represents the water obtained from the operation of fuel cell, R_{out} is the output power from the reformer, FC_{in} the input power to the fuel cell, and LHV_{H2} is the low heating value of hydrogen. Meanwhile, MW_{H2O} and MW_{H2} are the molecular weight of water and hydrogen, respectively.

In literature it is reported that water corresponds to 15-40% of the total mass of the digester [46]. Accordingly, in this work is considered a water consumption factor of 20%, i.e. 0.25 kgH_2O/kg biomass.

- *Inherent Safety:*

Power plants involve hazardous materials and processes that can lead to accidents, and negatively impact the health of workers and the wellbeing of communities. Therefore, aiming to avoid or reduce those accidents, a variety of methods can be implemented for evaluating the safety issue during the whole life cycle of the project [47]. Broadly, these methods differ in the aspects considered, the required information, and the output data type [43]. For example, some of the most common and popular approaches are the Hazard and Operability method (HAZOP), the Dow chemical/fire and exposure indices (C&EI and F&EI), and the Mond index [43,48]. However, these methods are not suitable for conceptual design stage, since they rely upon information from basic and detailed engineering such as the P&ID (piping and instrumentation diagram) of the process [43,47,48].

Moreover, some methodologies are based upon the assessment of the inherent safety of the processes. The essence of this perspective is to avoid and/or eliminate hazards rather than controlling them through add-on systems [49–52]. Indeed, these approaches rely on the fact that the potential risks of a process are related with the intrinsic characteristics of the chemical substances and operation units [52,53]. Inherent safety comprises four main principles: intensification, substitution, attenuation, and simplification. Intensification or minimization refers to quantities of materials and size of equipment within the plant. Thus, safer processes are those ones with lower number of hazardous substances and smaller operation units. Substitution relies on replacing hazardous materials for safer ones, e.g. using non-flammable and/or non-toxic refrigerants or solvents instead of flammable and/or toxic compounds.

Attenuation or moderation seeks to modify process conditions (e.g. temperature, pressure, concentration) for avoiding flammable limits or reactions close to runaway temperatures. Meanwhile, simplification lies on the fact that processes with less equipment lead to fewer opportunities for error, so that simpler plants are inherently safer [42,51,52].

Considering the foregoing, the inherent safety assessment is typically quantified as the contribution of two sub-indices: the chemical and the process inherent safety index. The former includes properties such as heat of reaction, flammability, explosiveness, and toxicity. In contrast, the latter focuses on process conditions such as pressure and temperature. In this respect, a variety of methods have been proposed to evaluate the inherent safety of processes. For example, Edwards and Lawrence proposed the prototype index of inherent safety (PIIS) which is mainly focused on the selection of raw materials and reaction steps [54]. Nonetheless, this is a reaction-oriented method and is not suitable for the safety evaluation of the whole process plant. In another work, Heikkilä proposed the inherent safety index (ISI), which allows comparison between different process alternatives [51]. Despite that, this method has some limitations because it is based on the worst-case scenario and does not consider neither the quantity of materials nor the amount of equipment within the process. Indeed, the evaluation of the worst-case scenario could lead to similar results even if considerably different processes are analyzed [53,55].

To overcome this issue, Li et al. proposed the enhanced inherent safety index (EISI), which includes all the chemicals and their amount by multiplying the flow rate with the severity factor (e.g. explosiveness or toxicity) [53]. Additionally, for the process inherent safety index, the scores of the equipment are multiplied by their number and are added all together. In a similar direction, recently Gangadharan et al. introduced the comprehensive inherent safety index (CISI) by adopting and object-oriented approach [55]. In this method, each equipment corresponds to a separate entity so that the inherent safety index is calculated for individual operation units. Moreover, this approach considers the severity of reactions based on the combination of chemicals, and a connection score between two units as a function of their individual safety scores.

In this work, the inherent safety for the energy system design is quantified based upon the comprehensive inherent safety index. However, the severity of reaction and the connection score are not included. The former because the score of reaction is considered as a function of the heat of reaction (already included), and the latter because that score could change depending on the judgement and/or experience of the method user, as stated by Gangadharan et al. [55]. Accordingly, the total inherent safety index for evaluating the energy system can be calculated by means of Equation 6. Moreover, Equation 7 describes the individual equipment

safety index, which includes the contribution of the chemical and process indices. The former is described by Equation 8 and the latter through Equation 9. Note that a lower index corresponds to a safer system structure.

$$IST = \sum_{k}^{K} I_{E,k} \tag{6}$$

$$I_{E,k} = I_{C,k} + I_{P,k} \tag{7}$$

$$I_{C,k} = \frac{\sum_{n}^{N}(I_{FL,n} + I_{EX,n} + I_{TOX,n} + I_{COR,n})F_n + I_{R,k}\sum_{n}^{N} F_n}{1000} \tag{8}$$

$$I_{P,k} = I_{I,k} + I_{T,k} + I_{Pr,k} \tag{9}$$

In those expressions, IST is the total inherent safety index, $I_{E,k}$ is the individual equipment safety index, $I_{C,k}$ is the chemical index, and $I_{P,k}$ is the process index of the equipment k. Additionally, $I_{FL,n}$, $I_{EX,n}$, $I_{TOX,n}$ and $I_{COR,n}$ are the flammability, explosiveness, toxicity and corrosiveness scores, respectively. F_n represents the mass flow rate, $I_{R,k}$ is the reaction sore, the subscript n denotes each chemical substance through the equipment k and the factor 1000 is the basis flow rate. Meanwhile, $I_{I,k}$, $I_{T,k}$ and $I_{Pr,k}$ correspond to the inventory, temperature, and pressure scores, respectively. Detailed information for computing the inherent safety index is presented in section S1 of the supplementary material. In this formulation is noted that the traditional scores for the inventory index ($I_{I,k}$) depicted in Table S7 are conceived to assess large-scale units. Nevertheless, as distributed energy systems are small-scale plants, in this work a new scale was proposed for the evaluation of that index. All the details of this analysis are presented in section S2 of the supplementary material.

2.3.2. Optimization Problem

Considering the two objective functions previously described, two independent optimization problems are stated to minimize the water consumption and the inherent safety index. The mathematical formulation of these problems was built following the approach developed by Fonseca et al. [44], which is presented in Equations 10-19.

$$Minimize \qquad J_1(u,x,t) = WC \tag{10}$$

$$J_2(u,x,t) = IST \tag{11}$$

$$Subject\ to \qquad h = f(u(t),x(t),p,t) \quad ,system\ model \tag{12}$$

$$0 \leq S_B(t) \leq S_{B,max} \quad ,battery\ storage \tag{13}$$

$$S_B(t_0) = S_B(t_f) \quad ,periodicity \tag{14}$$

$$0 \leq S_{H2}(t) \leq S_{H2,max} \quad , hydrogen\ storage \tag{15}$$

$$S_{H2}(t_0) = S_{H2}(t_f) \quad , periodicity \tag{16}$$

$$\int_{t0}^{tf} AD_{in}dt \leq Bio_D \quad , biomass\ available \tag{17}$$

$$0 \leq u(t) \leq 1 \ ; \ u \ni \{\varphi_1, \varphi_2, \theta_1, \alpha_1, \delta_1, \gamma_1\} \quad , optimization\ variables \tag{18}$$

$$\sum_{i}^{I} S_i(t) = 1 \quad S \ni \{\varphi, \theta, \alpha, \delta, \gamma\} \quad , consistency \tag{19}$$

Where, J represents each objective function and h the energy system model, which is a function of the decision variables (u), the state variables (x), the parameters (p), and the time (t). Moreover, the optimization problem also includes path (Equations 13 and 15) and endpoint (Equations 14 and 16) constraints on the level of energy stored in the battery (S_B) and in the pressurized tank (S_{H2}). The former to avoid negative values in the storage level, and the latter to ensure periodic behavior over the evaluated time horizon. Besides, Equation 17 represents a constraint for limiting the of biomass used in the digestion process according to the amount available (Bio_D). Meanwhile, Equation 18 denotes the set of optimization variables, which correspond to the fractions $\varphi_1, \varphi_2, \theta_1, \alpha_1, \delta_1$ and γ_1. Further details about the optimization approach and the energy system model can be found in reference [44].

The optimization problems were solved considering one year as time horizon and using time steps of 12 hours, i.e. $\Delta t = 12h$, $t_0 = 0h$ and $t_f = 8760h$. Likewise, the upper limits for the storage technologies are 30 and 300 MWh for the battery and the pressurized tank, respectively. Besides, the amount of biomass available (Bio_D) is 255.6 ton/year. This value was estimated by considering the domestic waste generated per inhabitant (568 kg/year), the fraction of organic matter that can be used in the digestion process (30%), and the size of the studied neighborhood (1500 inhabitants) [56,57]. Meanwhile, the photovoltaic surfaces evaluated in this work are 7500 and 10000 m^2. These values represent scenarios with an overcapacity of 50 and 100% with respect to the size required to cover the peak electricity demand [44].

2.4. Multi-objective Optimization

As stated in the introduction section, the multi-objective analysis proposed in this work considers the water consumption and the inherent safety index in addition to the total annualized cost, CO_2 emissions and grid dependence indicators previously used by Fonseca et al. [44]. Accordingly, five objective functions are included within the multi-objective optimization framework for the energy system design under the sustainability dimensions. The principles, criteria and indicators of the proposed framework are presented in Figure 2.

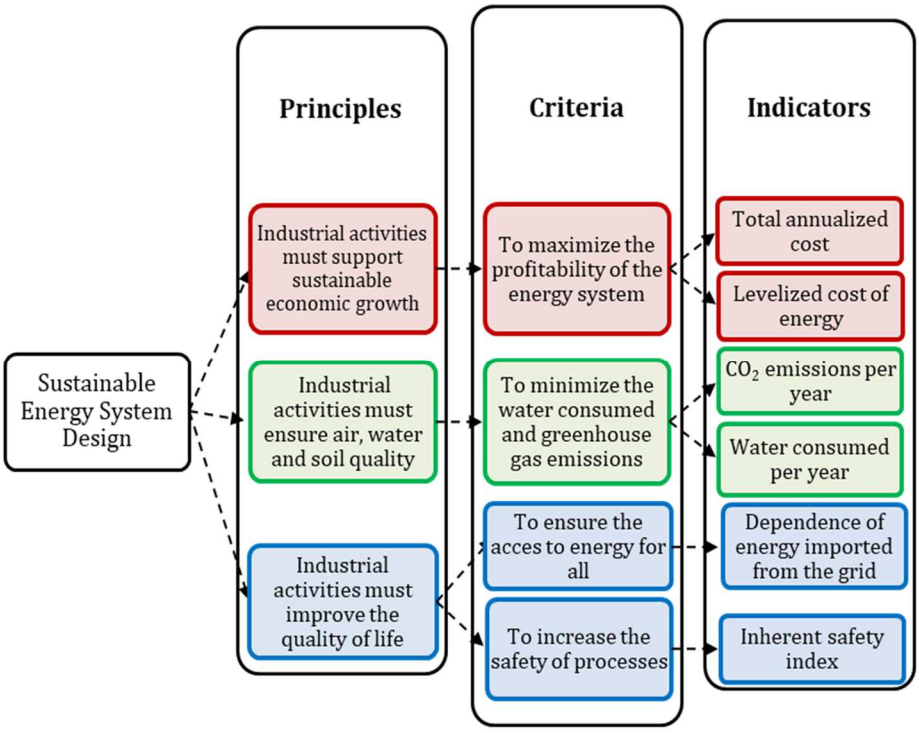

Figure 2. Framework of principles, criteria and indicators for the sustainability assessment of energy systems.

The results of an optimization problem including five objective functions would be hard to both visualize and analyze. Moreover, as presented in the introduction of this document (section 1.2), one of the goals of this work is to obtain a thorough understanding about the relationships among the objective functions and to identify some general insights for the conceptual design of DES. Accordingly, with the aim of performing this analysis, four multi-objective optimization problems are proposed and solved. These problems include different combinations of the indicators to assess the sustainability of the energy systems. The proposed cases cover the three dimensions of sustainability and simultaneously consider three objectives at most, which leads to results that can be clearly drawn in a three-dimension plot. Moreover, this strategy also enables to carry out a comprehensive analysis about the trade-offs of the objectives to support the subsequent decision-making process.

Table 2 depicts how the indicators are grouped for addressing the multi-objective optimization. As noted, each one of the problems involves at least two dimensions of sustainability. Thus, problem P1 includes two sub-problems, i.e. the cost against the CO_2 emissions and the cost against the grid dependence. This was selected as the first case because it covers the indicators previously analyzed in the literature. Meanwhile, problems P2 and P3 simultaneously include the three dimensions of sustainability and the two indicators introduced in this work (water consumption and inherent safety). Finally, problem P4 also comprises two sub-problems to complete the analysis among all the indicators, i.e. the safety against the cost, and the safety

against the CO_2 emissions are studied. The remainder of the formulation is identical to that employed in the single-objective optimization problems, i.e. Equations 12-19.

Table 2. Multi-objective optimization problems and corresponding indicators for the energy system design.

Problem	Indicators
P1	Cost - CO_2 emissions / Grid dependence
P2	Cost - Water consumption - Grid dependence
P3	Cost – Water consumption - Safety
P4	Safety – Cost / CO_2 emissions

A common strategy for solving multi-objective optimization problems is to transform the original problem into a single-objective one. That is the case of the weighting, epsilon-constraint, and global criterion methods. In general, such methods are simple and effective for solving problems with few objectives. However, they require to solve the optimization problem many times, since only one point of the Pareto set is obtained at a time. Moreover, as the number of objectives increases, it is more difficult to select suitable values for the weighting and epsilon-constraint methods [58,59].

Taking this into account and the number of sustainability indicators included in the proposed framework (5 objective functions), the Non-dominated Sorting Genetic Algorithm (NSGA-II) was selected for solving the proposed multi-objective optimization problems. This algorithm was used because it enables to simultaneously obtain the entire set of non-dominated solutions (i.e. only one optimization run is required), which provides more information to the decision-maker [58,60]. Besides, this evolutionary algorithm does not depend on continuity, derivative conditions and initial points, therefore it is suitable for solving problems that could be difficult to address with deterministic methods [60]. Moreover, the ready availability and effectiveness of the algorithm are well documented, as it has been extensively used to solve multi-objective optimization problems [58,60–62]. In this work, the NSGA-II algorithm was employed through the *gamultiobj* function within MATLAB® software.

3. Results and Analysis

3.1. Single-objective Optimization

Water consumption and inherent safety index were evaluated to enhance the analysis of the environmental and social dimensions of sustainability. Then, Figure 3 shows the optimal flowsheet of the system by optimizing those objectives.

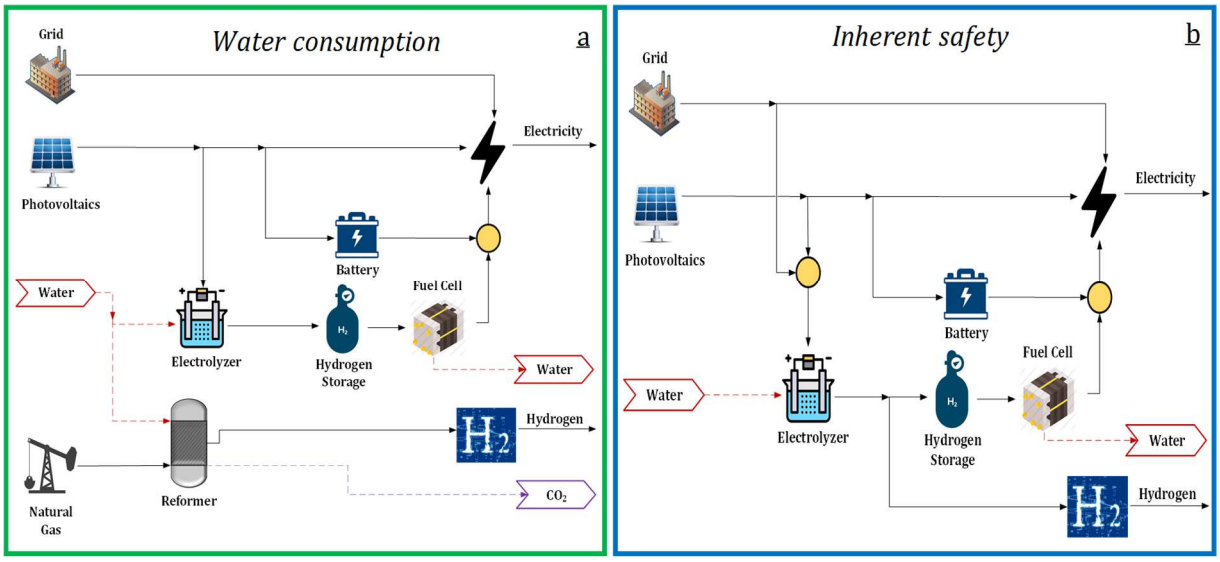

Figure 3. Optimal configurations of the distributed energy system. Objective functions (a) water consumption, (b) inherent safety index.

Regarding the minimization of water consumption, the obtained system configuration indicates that the electrolyzer is only powered by PV electricity, and that all the hydrogen produced by this process is sent to the pressurized tank, as observed in Figure 3a. Therefore, the whole demand of hydrogen is supplied by the steam methane reforming process. Also note that the anaerobic digester is not included within the system, hence, only methane from the main network is supplied to the reformer reactor.

On the one hand, the fact of sending all electrolytic hydrogen to the storage tank can be explained by analyzing the Equation 3. In that expression, it is noted that the employment of the system electrolyzer-tank-fuel cell offers the possibility of recovering the water produced in the fuel cell to be reused in the electrolyzer. In contrast, if such hydrogen is sent to supply the demand, there is no way of recuperating the water, and therefore its net consumption will increase. On the other hand, the selection of reforming instead of electrolysis process lies on the stoichiometry of reactions. Thus, by considering the stochiometric relation of each process, water electrolysis requires 9 kgH_2O/kgH_2, whereas the reforming reaction needs 4.5 kgH_2O/kgH_2. Consequently, as the objective is to minimize the water consumption, steam reforming process provides a better performance than water electrolysis.

Otherwise, concerning the optimization of the inherent safety index, the obtained results indicate that the whole demand of hydrogen must be supplied by the water electrolysis process, as depicted in Figure 3b. Thus, neither the reformer nor the anaerobic digester is included within the energy system. This happens because one of the principles of the inherent safety lies on the simplification of the process, so that a safer process is the one with less amount of equipment. In such a way, as the electrolyzer is already installed for converting the surplus

electricity into hydrogen, it is used to produce all the required hydrogen. In fact, even though the electrolyzer was not employed as part of the storage system, it would be the preferred option for obtaining hydrogen instead of the reformer. This fact can be verified by comparing the operating conditions of the two processes. In this respect, the electrolyzer typically operates at 80°C and 4 MPa, whereas the reforming reaction is carried out at 800°C and 3 MPa.

Table 3. Optimization results of the distributed energy system for minimizing the water consumption (WC) and the inherent safety index (IST).

Variable	PV area = 7500 m^2		PV area = 10000 m^2	
	WC	**IST**	**WC**	**IST**
LCOE (€/kWh)	0.57	0.54	0.63	0.58
TAC (M€/year)	2.7	2.6	3.0	2.8
CAPEX (% TAC)	92	90	94	92
OPEX (% TAC)	8	10	6	8
CO_2 emissions (ton/year)	329.5	124.7	310.3	89.3
Grid emissions (%)	33	100	29	100
Process emissions (%)	67	-	71	-
Biogenic (ton/year)	-	-	-	-
Water consumption (m^3/year)	134.1	276.7	193.4	313.6
Electrolysis (%)	26	100	51	100
Reforming (%)	74	-	49	-
Digestion (%)	-	-	-	-
Grid Dependence (%)	49	44	42	30
Imported electricity (%)	39	100	29	100
Imported natural gas (%)	61	-	71	-
Inherent Safety	23.0	12.1	23.8	13.4
Chemical Index	1.8	1.5	2.5	2.2
Process Index	21.2	10.6	21.3	11.2

Table 3 presents the main results for the five sustainability indicators when the water consumption and the inherent safety index are minimized. Moreover, these results also depict the impact of the PV surface on the objective functions. In this respect, it is noted that the performance of both indicators improves as the area of PV decreases. Regarding the water consumption, it occurs because a larger PV surface leads to a higher amount of surplus electricity, and consequently more water is required for converting such excess of electricity into hydrogen for its storage. Similarly, the energy system becomes safer as the size of the PV decreases, since smaller equipment are needed for energy conversion and storage.

3.2. Multi-objective Optimization

As aforementioned, the multi-objective optimization framework proposed in this work includes five objective functions. Therefore, aiming to summarize the results from the single-objective optimization, and to ease the analysis of the multi-objective optimization problems, Figure 4 depicts the obtained energy system configuration from the independent assessment of each one

of the five objective functions. It is noteworthy that the flowsheets corresponding to the economic, CO_2 emissions and grid dependence indicators were taken from the reference [44].

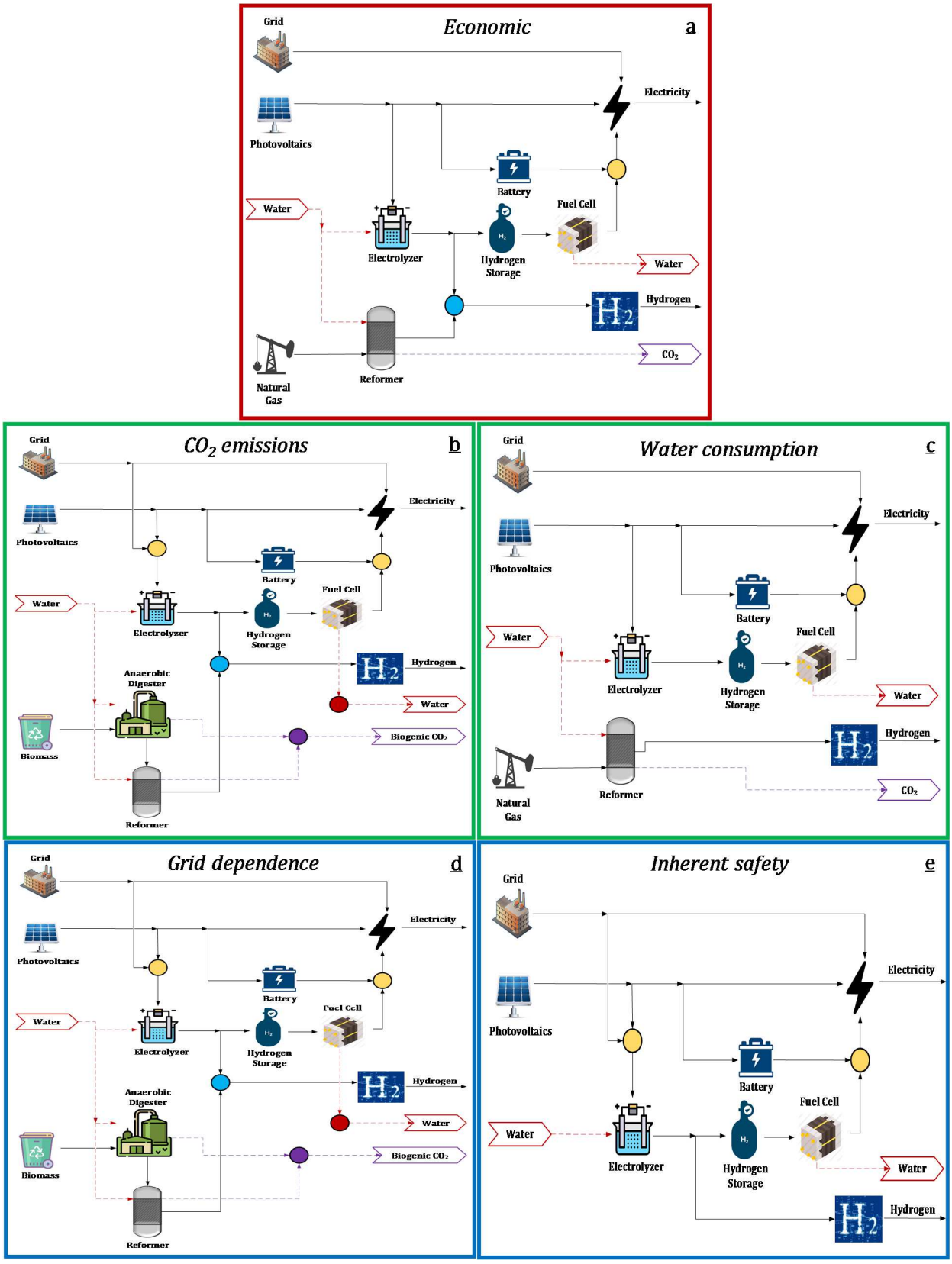

Figure 4. Optimal configurations of the distributed energy system from single-objective optimization. Objective functions (a) total annualized cost, (b) CO_2 emissions, (c) water consumption, (d) grid dependence, (e) inherent safety index.

3.2.1. Problem 1: Cost - CO_2 emissions/grid dependence

Figure 5 depicts the Pareto fronts for the two multi-objective optimization problems: (i) economic-environmental (Figure 5a), and (ii) economic-social (Figure 5b). Initially, such problems were solved considering different sizes of the population for the genetic algorithm. In this respect, populations between 500 and 4000 individuals were evaluated to identify the impact of this variable on the Pareto solutions. The corresponding results are presented in Figures S2 and S3 of the section S3 in the supplementary material. Accordingly, a population of 3000 individuals was selected, since for populations larger than 2000 individuals, no significant impact of this variable was observed on the optimal set of solutions.

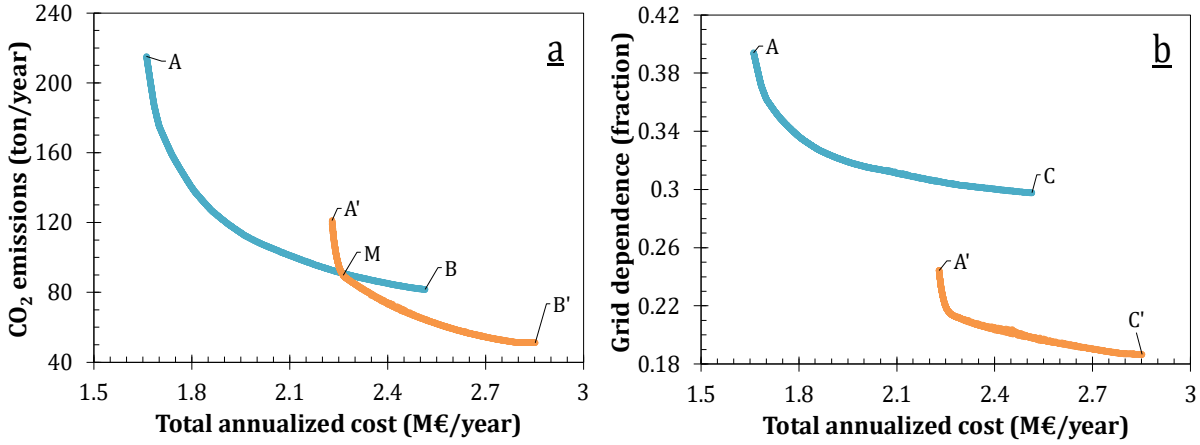

Figure 5. Pareto fronts for the distributed energy system design. (a) CO_2 emission - cost, (b) grid dependence – cost. Photovoltaic surface (●) 7500 m², (●) 10000 m². (A – A') optimal cost, (B – B') optimal emission, and (C – C') optimal grid dependence.

First, note that the points A-A' correspond to the best performance from the economic point of view, the points B-B' represent the best solution from the environmental perspective, and the points C-C' represent the minimal grid dependence. Thus, the obtained Pareto fronts reflect the competitive behavior of both pair of objectives, since as the total annualized cost decreases, the CO_2 emissions and the grid dependence get worse.

Moreover, Figure 5 also depicts the influence of the PV surface on the Pareto solutions. In this respect, a larger area of PV enables to achieve lower CO_2 emissions and grid dependence, but it also entails a greater economic cost. In general, these results provide a wide range of solutions that can be further evaluated for the decision-maker to their implementation. Interestingly, the results show that there is a zone wherein the PV surface of 7500 m² will not be competitive

against the area of 10000 m^2. This occurs for the solutions between the points B and M because all of them could be improved in at least one criterion by using a PV surface of 10000 m^2. Mathematically, this implies that the solutions within the MB line are dominated by those obtained with a PV area of 10000 m^2 (line A'B'). In such a way, if the decision-maker is willing to invest between 2.3 and 2.5 M€, it would be better to install a PV surface of 10000 instead of 7500 m^2, since for the same cost lower CO_2 emissions and grid dependence could be obtained.

Comparing the energy system configuration for the extreme points of the Pareto front, i.e. those obtained from the mono-objective optimization (Figure 4), it is noted that the difference of the energy system structure lies on the source of methane for the reforming process. Thus, when the economic objective is addressed, all the methane is imported from the network (Figure 4a). In contrast, if the objective is to reduce the CO_2 emissions or the grid dependence, the reformer reactor is fed by methane from the anaerobic digestion process (Figures 4b and 4d).

Aiming to elucidate the differences in the design and operating conditions throughout the Pareto fronts, Figure 6 presents the installed size and the use of some energy sources as a function of the total annualized cost. As noted in Figures 6a and 6b, there is a direct relation between the energy storage capacities and the total cost of the system. Therefore, the best configurations from the economic perspective correspond to those with the smallest storage units. Meanwhile, Figures 6c and 6d depict the change in the source of methane for the reforming process. As observed, the best performance for the CO_2 emissions and grid dependence indicators is obtained without importing methane from the grid and by using the maximum amount available of biomass. Then, as the economic performance improves, the imported natural gas increases and the biomass gets unused, but at the cost of higher CO_2 emissions and grid dependence. Interestingly, note that whilst the storage capacities are the most influencing variables on the cost criterion, the source of methane has the biggest impact on the emission and grid dependence issues. This fact can be observed by analyzing Figures 5 and 6. In such a way, going from low emission to low cost, it is observed that the most significative alteration on the slope of the Pareto curves corresponds to an important change in the curves of the imported natural gas and the biomass consumption. Roughly, this occurs at a value of 1.9 M€ for a PV surface of 7500 m^2, and at 2.2 M€ when the area of PV is 10000 m^2. Moreover, it is also noted that the biomass utilization does not seem to have a great impact on the economic indicator (Figure 6d).

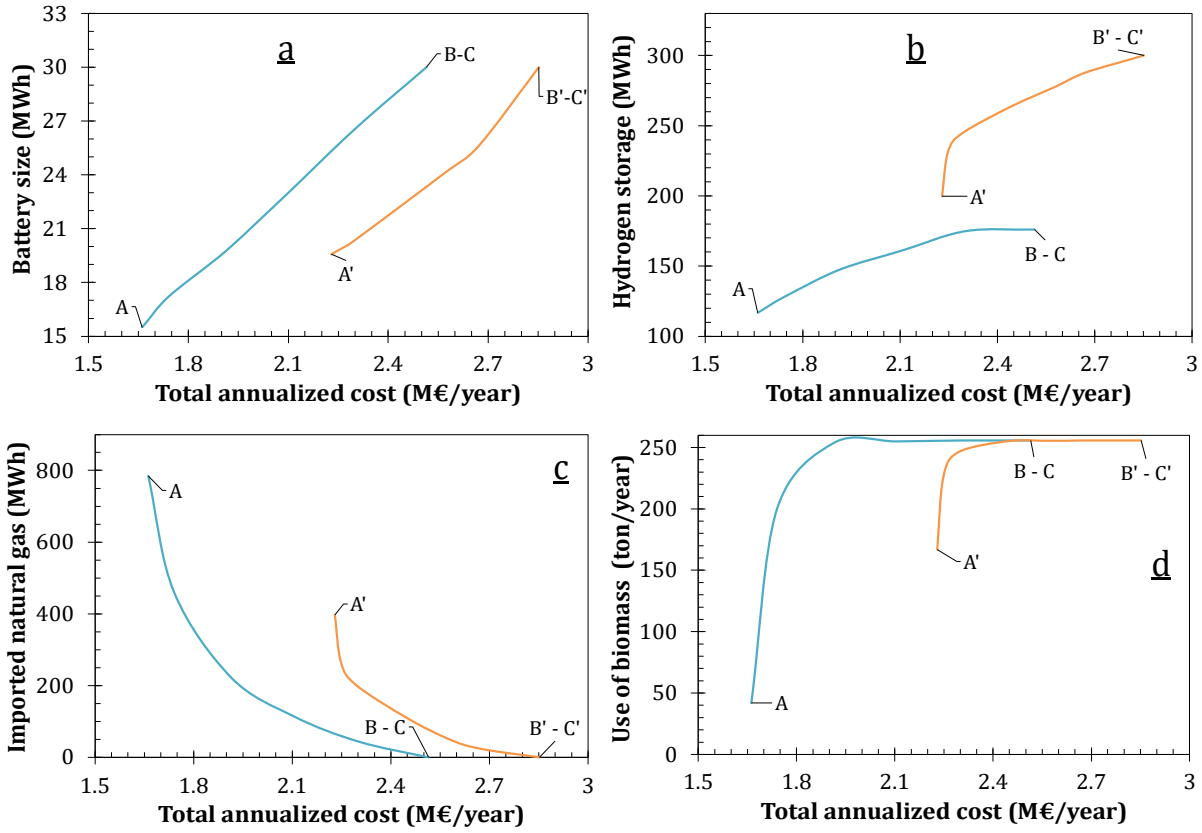

Figure 6. Change of design and operation conditions across the Pareto fronts. Photovoltaic surface (—) 7500 m² and (—) 10000 m². (a) battery, (b) pressurized tank, (c) imported natural gas, and (d) biomass consumption. (A – A') optimal cost, (B – B') optimal emission, (C – C') optimal grid dependence.

3.2.2. Problem 2: Cost - water consumption - grid dependence

The second multi-objective optimization problem consisted in the simultaneous minimization of the total annualized cost, water consumption and grid dependence. Initially, the problem was solved considering different sizes of population for the genetic algorithm. According to the obtained results, a population of 3000 individuals was selected, since above 2000 individuals, no significant effect on the Pareto solutions was observed. Results of such optimizations are presented in Figure S4 of the supplementary material. Accordingly, Figures 7 and 8 depict the obtained Pareto sets considering a PV surface of 7500 and 10000 m², respectively. Such figures include a 3-dimension representation (Figures 7a and 8a), and the 2-dimension projections for the three evaluated objectives.

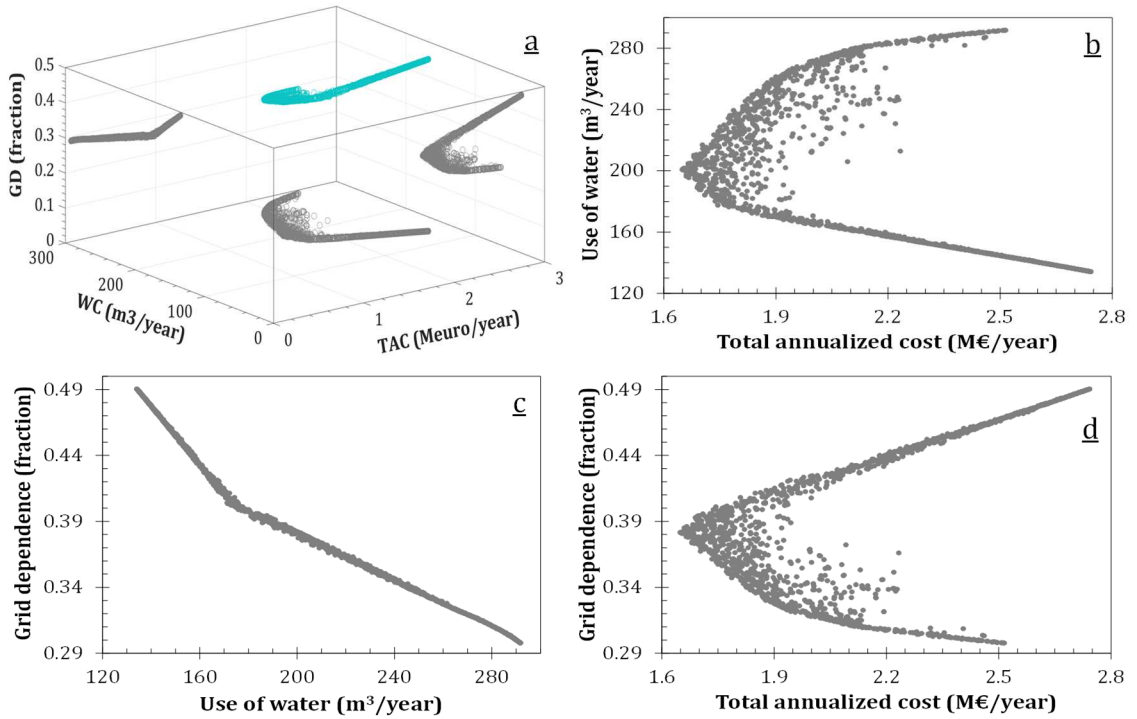

Figure 7. Pareto solutions for minimizing the total annualized cost, the water consumption and the grid dependence considering a photovoltaic surface of 7500 m^2. (●) 3-dimension representation (●) 2-dimension projections.

Results show the trade-offs and the relationships among the objective functions. In fact, the competition among the three indicators can be observed. Thus, the minimum water consumption implies the poorest yield in the cost and self-sufficiency indicators. In the same line, the lowest grid dependence requires the greatest water consumption. According to optimization results, it is also noted that for a given value of the economic indicator (TAC), there is a wide range of possible energy system structures and/or operating policies (Figures 7b, 7d, 8b and 8d). Then, for a fixed cost, the selection of the preferred alternative would require defining a value for the water consumption or the grid dependence. Figures 7c and 8c depict the relation between these two objectives. In this respect, the decision would depend on the specific context conditions and/or decision-maker preferences considering the reliability of the grid and the availability of water. For instance, if the energy system is developed in an isolated location or with regular energy outages, the grid dependence indicator must be privileged to assure the access to energy. Meanwhile, if the project is implemented in an arid zone, or in a place with low water resources, the indicator related to the water consumption will be the most important in the selection of the energy system.

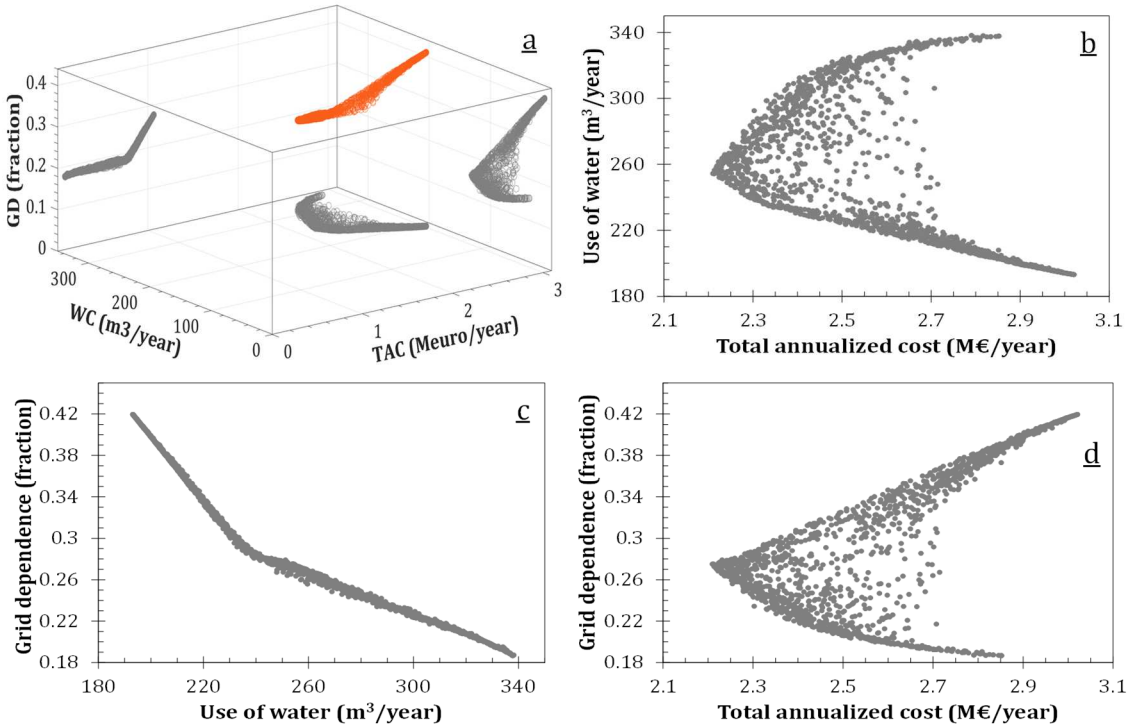

Figure 8. Pareto solutions for minimizing the total annualized cost, the water consumption and the grid dependence considering a photovoltaic surface of 10000 m². (●) 3-dimension representation (●) 2-dimension projections.

Figure 9 presents the comparison of the Pareto solutions for the two evaluated areas of PV . In those figures, the points A-A', B-B' and C-C' represent the optimal value of the economic, environmental, and social objectives, respectively. In general, the results suggest that the total annualized cost and water consumption indicators improve as the PV surface decreases. Conversely, larger areas of PV favor the energy autonomy. In this respect, note that as the PV surface gets larger, the surplus of electricity increases, and consequently, there is a need of bigger units for energy storage. For the economic and environmental objectives, this implies higher investment cost due to the size of equipment, and more elevated use of water for converting the surplus electricity into hydrogen through the electrolyzer. In contrast, as the area of PV becomes larger, the grid dependence indicator is enhanced, since in such a case, there is a greater amount of energy available from renewable sources, and therefore less energy must be imported from the grid.

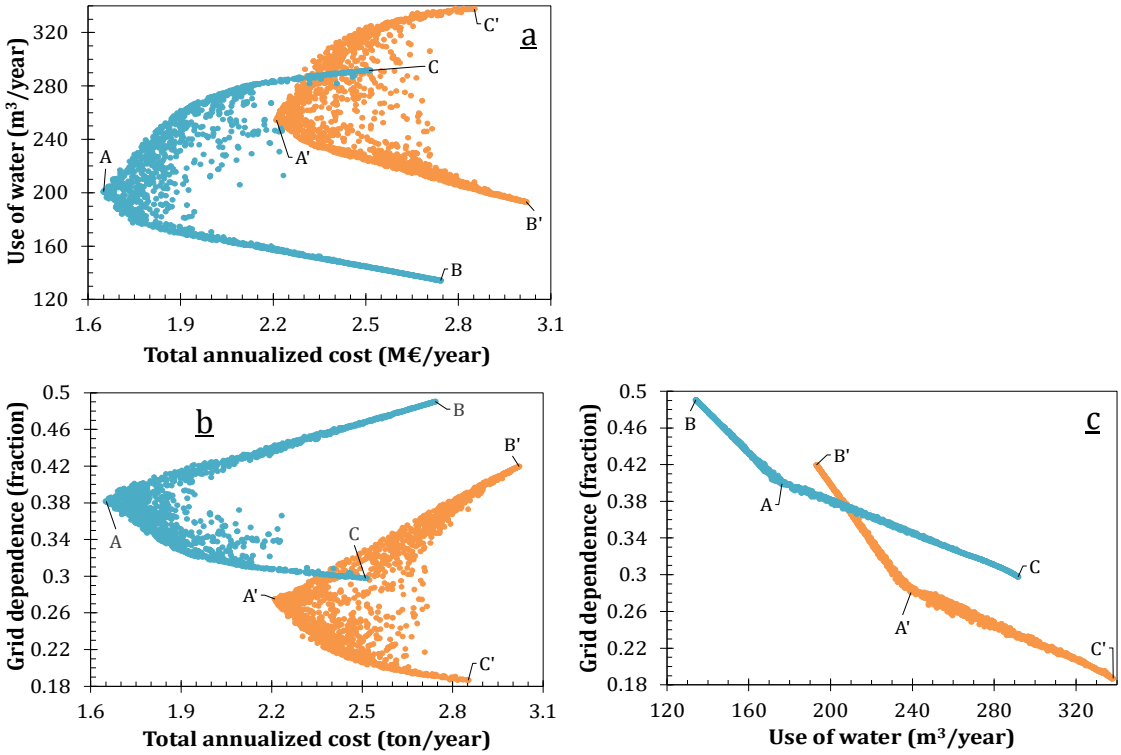

Figure 9. 2-dimension projection of the Pareto solutions for minimizing the total annualized cost, the water consumption, and the grid dependence. Photovoltaic surface (●) 7500 m², (●) 10000 m². (A – A') optimal cost, (B – B') optimal water consumption, (C – C') optimal grid dependence.

Comparing the optimal configuration from the economic (Figure 4a) and environmental perspectives (Figure 4c), note that both structures involve the same set of equipment for energy conversion and storage. Indeed, according to the flowsheets, the only difference is in the sources for supplying the hydrogen demand. Thus, whilst the economic optimization includes the possibility of providing hydrogen from water electrolysis, the water consumption indicator suggests that all the hydrogen must be supplied via steam methane reforming. In this respect, Figure 10 shows the change in the design and operation parameters by going from the economic (A-A') to the environmental (B-B') indicator across the Pareto solutions. On the one hand, as observed in Figures 10a and 10b, the economic optimum corresponds to the configurations with the smallest size of the storage units. This happens because such devices represent about 60-65% of the CAPEX of the system [44].

On the other hand, note that moving towards the optimal value of the water consumption requires to increase the capacity of energy storage (Figures 10a and 10b) and the amount of natural gas imported from the network (Figure 10c). Regarding the energy storage issue, it can be explained by the fact that when the whole system electrolyzer-tank-fuel cell is employed, there is a possibility to recover the water produced in the fuel cell to be reused in the electrolyzer. Consequently, the net water consumption is lower than that obtained by sending

the hydrogen to supply the demand. Besides, the requirement of methane for the reforming process increases as moving towards the minimal water consumption (points B and B'), since the hydrogen supplied by water electrolysis gets lower.

Moreover, the best performance for the grid dependence indicator is obtained by feeding the reforming reactor with only the biomethane produced from the anaerobic digestion process (Figure 4d). Accordingly, this configuration corresponds to that without importing natural gas from the network and with the highest use of biomass, as presented by the points C-C' in the Figures 10c and 10d.

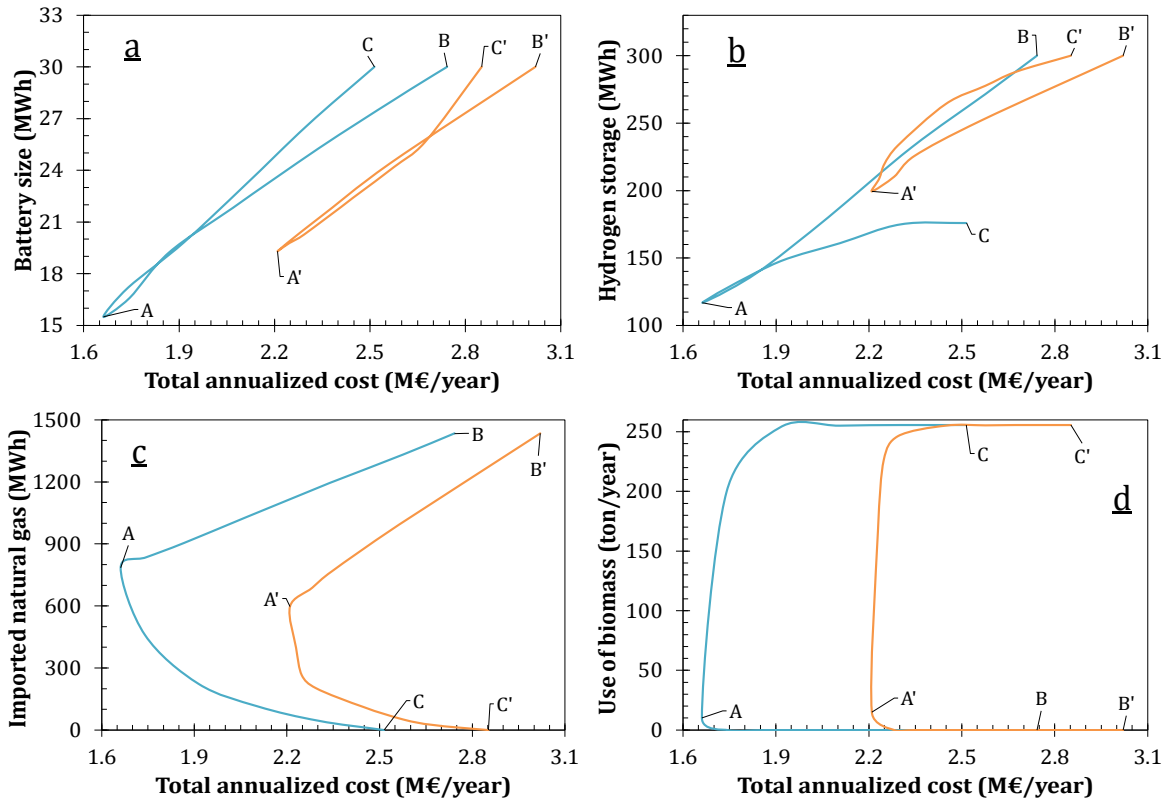

Figure 10. Change of design and operation conditions across the Pareto solutions. Photovoltaic surface (—) 7500 m² and (—) 10000 m². (a) battery, (b) pressurized tank, (c) imported natural gas, and (d) biomass consumption. (A – A') optimal cost, (B – B') optimal water consumption, (C – C') optimal grid dependence.

3.2.3. Problem 3: Cost – water consumption - safety

In this optimization problem, the three dimensions of sustainability are evaluated by means of the total annualized cost, water consumption and inherent safety indicators. As before, the first step consisted in performing the optimization by considering different sizes of population for the genetic algorithm. In this case, the evaluated values were 500 and 2000 individuals, and according to the obtained results, no considerable effect of this variable on the set of Pareto solutions was observed. Such results are depicted in Figure S5 of the supplementary material. Consequently, the results corresponding to a population of 2000 individuals were selected for

analyzing the multi-objective optimization problem. Then, Figures 11 and 12 present the obtained Pareto solutions considering a PV surface of 7500 and 10000 m^2, respectively.

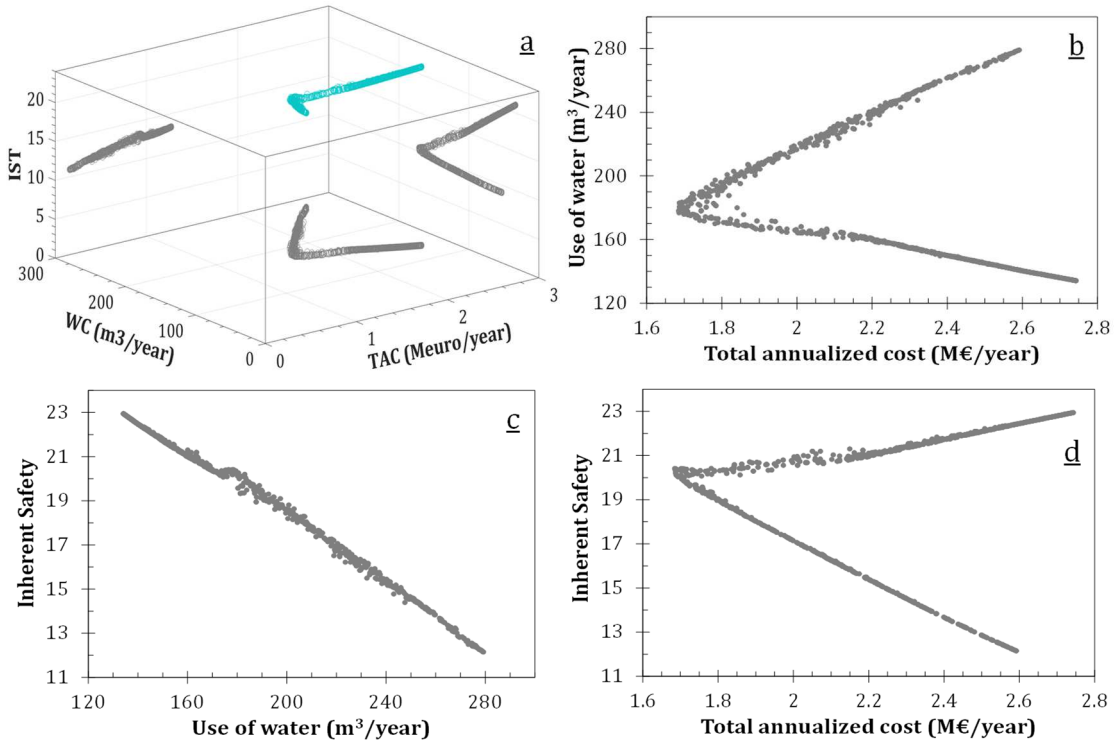

Figure 11. Pareto solutions for minimizing the total annualized cost, the water consumption and the inherent safety considering a photovoltaic surface of 7500 m^2. (●) 3-dimension representation (●) 2-dimension projections.

In general, results show the compromise among the objective functions and their contradictory behavior. As depicted in Figures 11(12)b and 11(12)d, there are at least two feasible energy system configurations or operating conditions that yield the same performance in the economic indicator. In such a way, the choice of the most suitable option involves the evaluation of the trade-off between the water consumption and safety indicators, which is presented in Figures 11(12)c. In those figures, the competition between these two objectives can be noted since the improvement of the safety index requires to increase the use of water.

Moreover, Figure 13 illustrates the obtained Pareto solutions for the two assessed areas of PV. In those figures, the points A-A', B-B' and C-C' represent the optimal value of the economic, environmental, and social objectives, respectively. As mentioned in a previous multi-objective optimization problem (P2), the total annualized cost and water consumption indicators improve as the PV surface decreases. Likewise, the safety indicator also gets better for the smallest size of PV, as shown in Figures 13b and 13c. As aforementioned (P2), as the surface of PV increases, bigger units are required for converting the surplus electricity into hydrogen and for energy storage. Consequently, this leads to an energy system with higher costs, more elevated consumption of water, and more hazardous conditions.

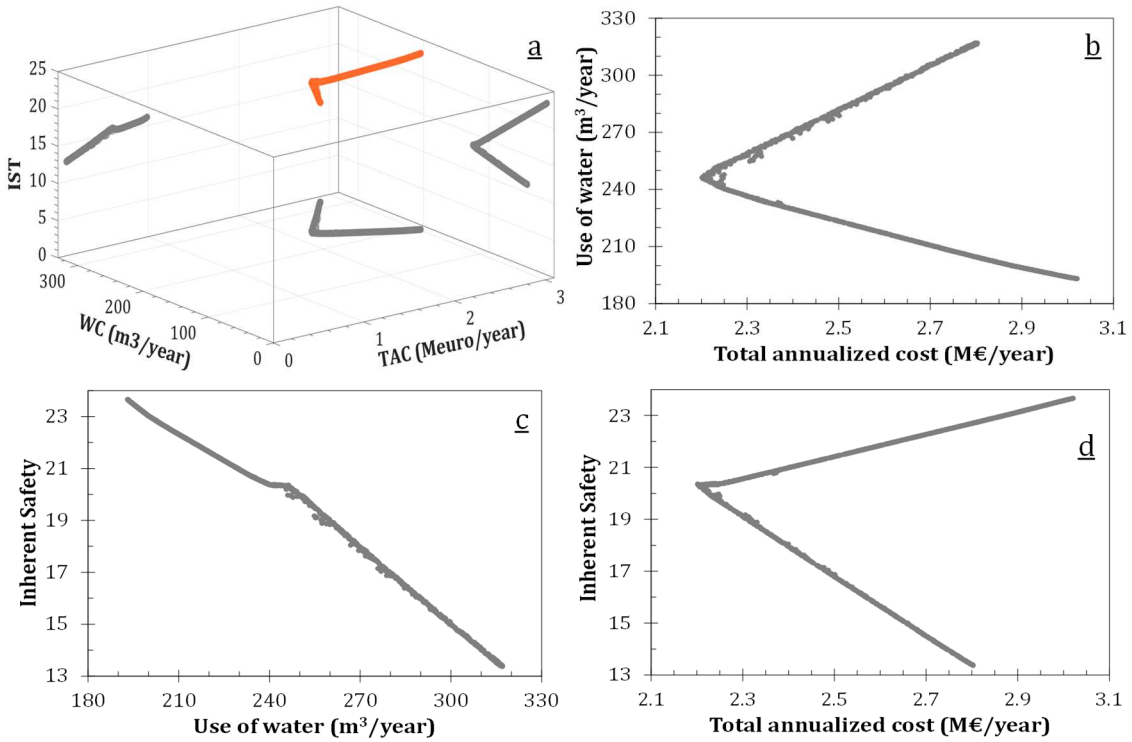

Figure 12. Pareto solutions for minimizing the total annualized cost, the water consumption and the inherent safety considering a photovoltaic surface of 10000 m². (●) 3-dimension representation (●) 2-dimension projections.

The comparison between the results of the economic and water consumption indicators was already discussed in the optimization problem P2. Meanwhile, note that the optimization of the safety index implies a new alternative for the energy system configuration (Figure 4e). In this regard, aiming to reduce the amount of equipment, the safety indicator suggests a process flowsheet without the reforming reactor. This result can be explained by two facts: (i) because of the intense operating conditions of the reforming process (temperature and pressure), and (ii) because the electrolyzer is already installed as a part of the hydrogen storage system. Likewise, as the reformer is not used, connection with the natural gas network is not required, since all the hydrogen is obtained via water electrolysis. Additionally, according to the results, the electrolyzer must be powered by both the PV and the electricity grid.

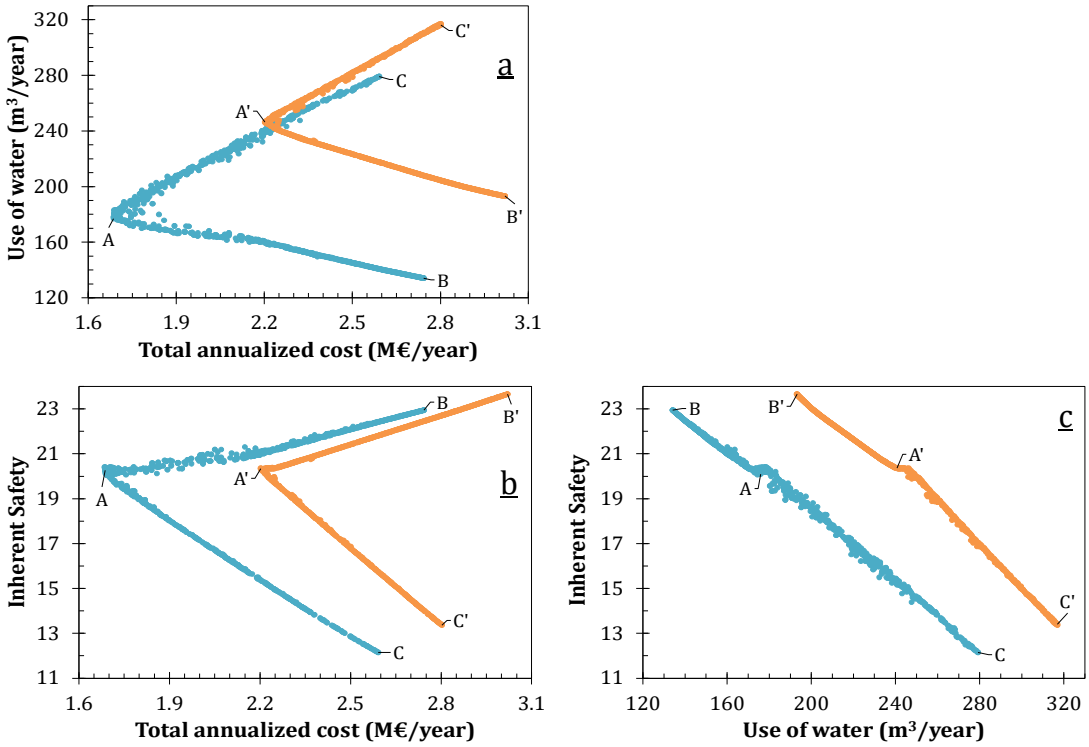

Figure 13. 2-dimension projection of the Pareto solutions for minimizing the total annualized cost, the water consumption, and the inherent safety. Photovoltaic surface (●) 7500 m², (●) 10000 m². (A – A') optimal cost, (B – B') optimal water consumption, (C – C') optimal inherent safety.

Figure 14 illustrates the changes in design and operating conditions across the Pareto solutions. Going from the economic (A – A') to the safety optimum (C – C'), it is noted that the capacity of the battery increases (Figure 14a), whereas the size of the pressurized tank gets smaller (Figure 14b). This happens because in improving the safety of the process, the system seeks to reduce the inventory of material (hydrogen) as much as possible, and consequently the battery becomes used more for storing the surplus electricity. Also, by moving towards the safest energy system configuration, the reforming reactor gets unused, and hence its installed capacity decreases (Figure 14c). At the same time, the electrolyzer is gradually more used for supplying the demand of hydrogen, and consequently, the requirement of importing electricity from the grid increases, as depicted in Figure 14d.

Interestingly, as shown in Figures 13b and 13c, the greatest change on the safety index occurs between the economic and social points, i.e. lines AC and A'C' of those figures. Indeed, note that there is a change in the slope of the curves in Figure 13c after the points A and A'. This can be explained by the results depicted in Figures 14b and 14c. As observed, whilst the capacity of the pressurized tank decreases across the lines BA and B'A', the size of the reformer remains constant. This implies that in that zone only the size of the pressurized tank affects the safety index, which translates into the smaller effect presented in Figures 13b and 13c. Conversely, in

the region represented by lines AC and A'C', the capacity of both the pressurized tank and the reformer reactor decreases, which leads to a bigger impact on the safety of the system.

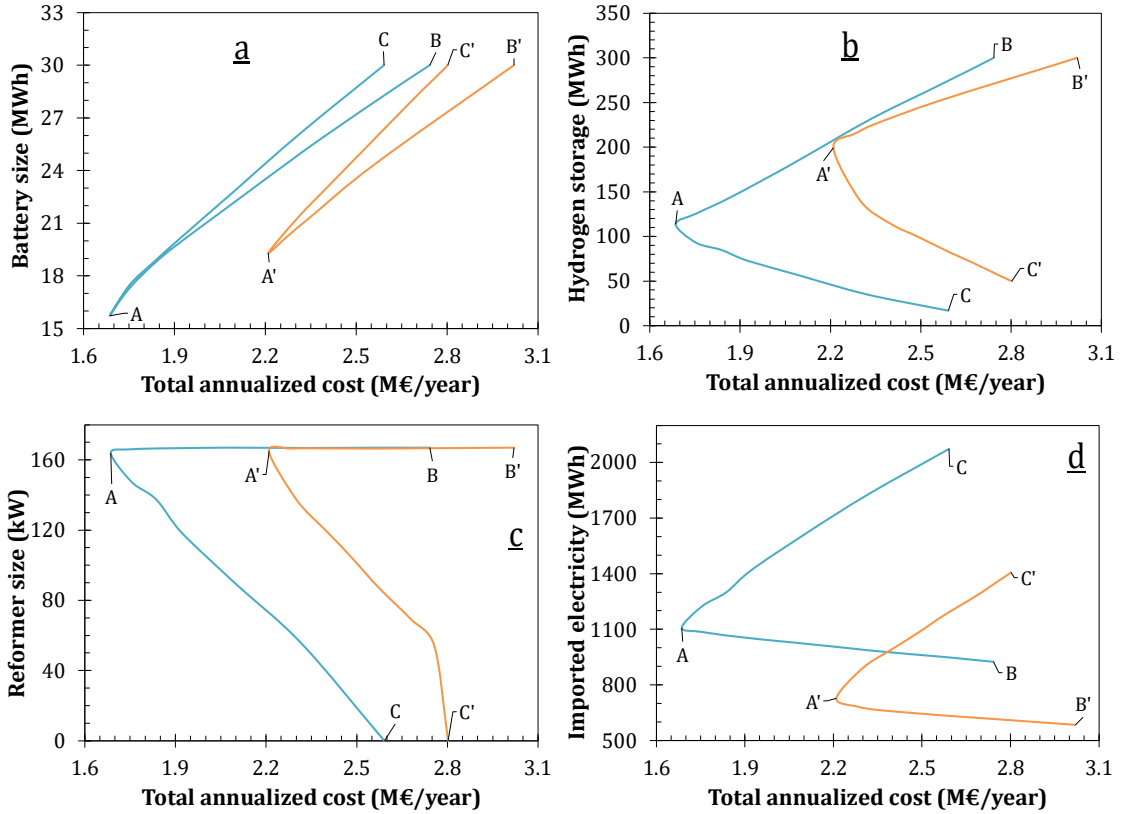

Figure 14. Change of design and operating conditions across the Pareto solutions. Photovoltaic surface (—) 7500 m² and (—) 10000 m². (a) battery, (b) pressurized tank, (c) imported natural gas, and (d) imported electricity. (A – A') optimal cost, (B – B') optimal water consumption, (C – C') optimal inherent safety.

3.2.4. Problem 4: Safety – cost/CO_2 emissions

This case comprises two multi-objective optimization problems: (i) the inherent safety against the total annualized cost, and (ii) the inherent safety against the CO_2 emissions. As before, these problems were solved by using a variety of sizes of population for the genetic algorithm. The values considered were 1000, 2000 and 3000 individuals. Results of these optimizations are presented in Figures S6 and S7 of the supplementary material. According to those results, a population of 2000 individuals was selected for analyzing the multi-objective optimization problems. Figure 15 depicts the obtained Pareto front for both optimization cases and the two surfaces of PV evaluated.

Results show the antagonistic behavior of inherent safety index with respect to both the total annualized cost and the CO_2 emissions. Therefore, as the hazardous of the energy system decreases, the cost of the plant (Figure 15a) and the emissions (Figure 15b) become higher. Figure 15 also shows the influence of the PV surface on the Pareto fronts. In this respect, note

that the inherent safety improves as the area of PV decreases. This happens because a smaller PV surface enables to reduce the size of the energy conversion and storage units, which favors the safety of the system.

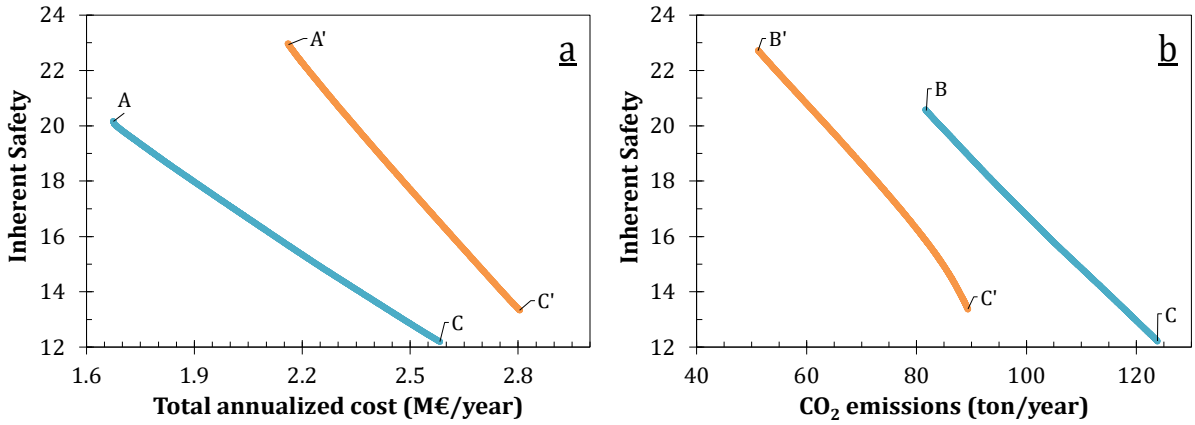

Figure 15. Pareto fronts for optimizing the total annualized cost, the CO_2 emissions, and the inherent safety. (a) safety - cost, (b) safety – CO_2 emissions. Photovoltaic surface (●) 7500 m², (●) 10000 m². (A – A') optimal cost, (B – B') optimal emission, and (C – C') optimal inherent safety.

As observed by comparing the Figures 4a, 4b and 4e, the topology of the system mainly differs in the energy sources employed for supplying the demand of hydrogen. Thus, the economic objective focuses on producing hydrogen from two process options: (i) the steam methane reforming (using the gas network), and the water electrolysis powered by PV (Figure 4a). Meanwhile, the CO_2 emissions indicator suggests including the anaerobic digester for obtaining biogas and subsequently perform the reforming process (Figure 4b). Besides, in this case, the electrolyzer is powered by both the electricity grid and the PV. Unlike, the inherent safety index does not include the reforming process within the energy system (Figure 4e).

Aiming to elucidate the relation of the optimization objectives in terms of design and/ or operating conditions, Figure 16 presents the evolution of these variables across the Pareto fronts. As mentioned in the optimization problem P3, the relation between the cost and safety indicators can be explained through two process aspects: the size of the units for energy storage, and the sources of hydrogen. In this regard, as noted in Figure 16a, the economic objective attempts to reduce the capacity of the battery because of its high investment cost. In contrast, the safety indicator focuses on reducing the amount of hydrogen stored (Figure 16c), and the size of the reformer because of its intense operating conditions (Figure 16e). Therefore, moving from the safest to the economical energy system requires to increase the capacity of the pressurized tank, to install and expand the capacity of the reforming reactor, and to decrease the size of the battery.

On the other hand, the right column in the Figure 16 shows the changes of the energy system when the CO_2 emissions and the safety indicators are addressed. Again, the safety index seeks to reduce capacity of the pressurized tank, whereas the environmental indicator requires a large storage capacity for exploiting the energy production from renewables (Figure 16b). Moreover, as the safety of the system increases, the electrolyzer becomes the preferred alternative to obtain hydrogen. Accordingly, the amount of electricity imported from the grid gets higher, as depicted in Figure 16d. Thus, as the CO_2 emissions grow, the anaerobic digester and reformer reactor get unused, and hence the use of biomass decreases (Figure 16f).

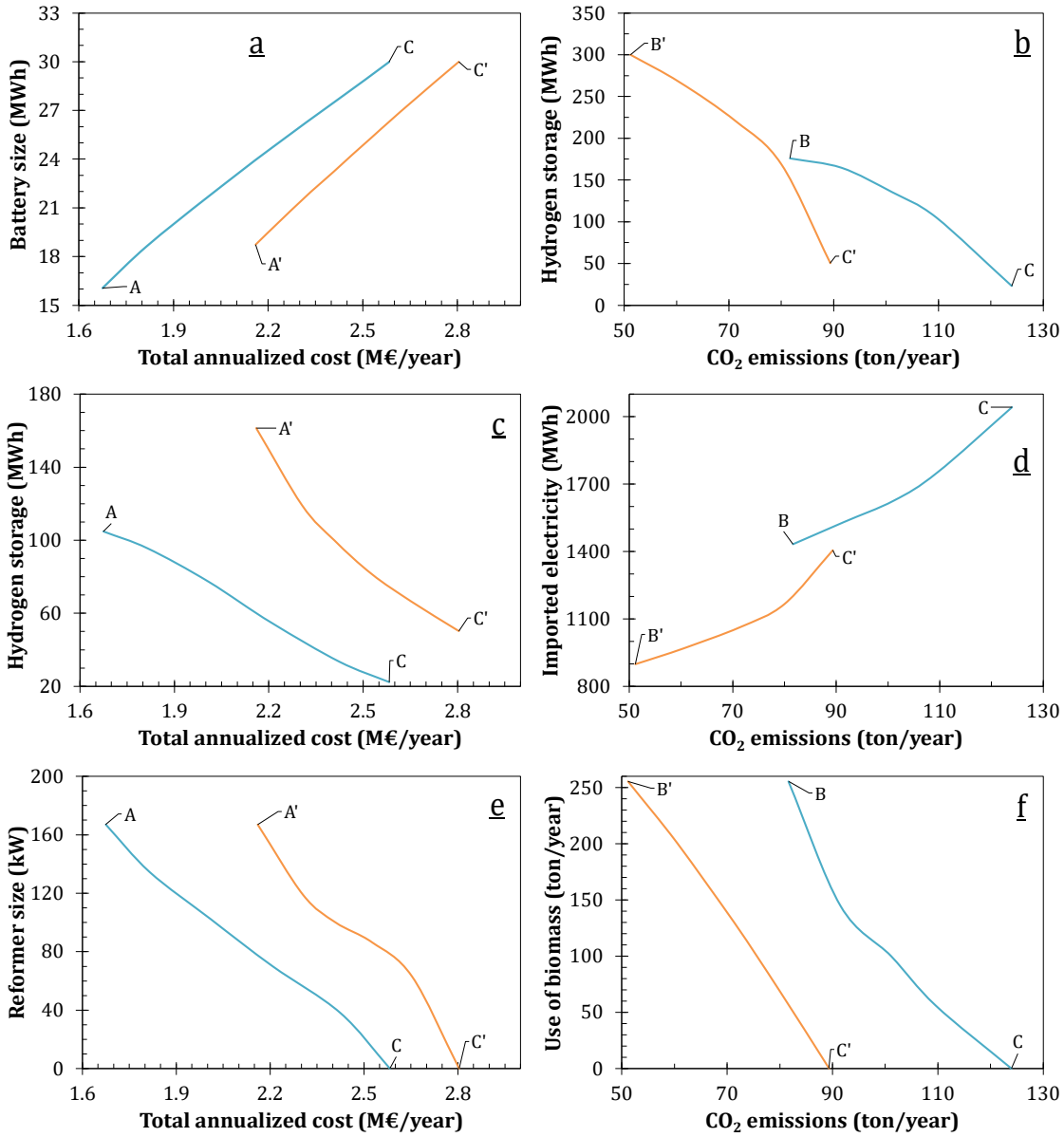

Figure 16. Change of design and operating conditions across the Pareto fronts. Photovoltaic surface (—) 7500 m² and (—) 10000 m². Left column (a,c,e) cost vs inherent safety, right column (b,d,f) CO_2 emissions vs inherent safety. (A – A') optimal cost, (B – B') optimal emission, and (C – C') optimal inherent safety.

4. General Insights for the Design of DES

Throughout the previous section, different multi-objective optimization problems were addressed for the energy system design considering the sustainability dimensions. Besides, the obtained Pareto sets were explored for studying the compromises among the criteria, and the evolution of the process variables across the non-dominated solutions. Accordingly, aiming to summarize those findings, this section is dedicated to state the main trends and to identify some general insights for the conceptual design of distributed energy systems.

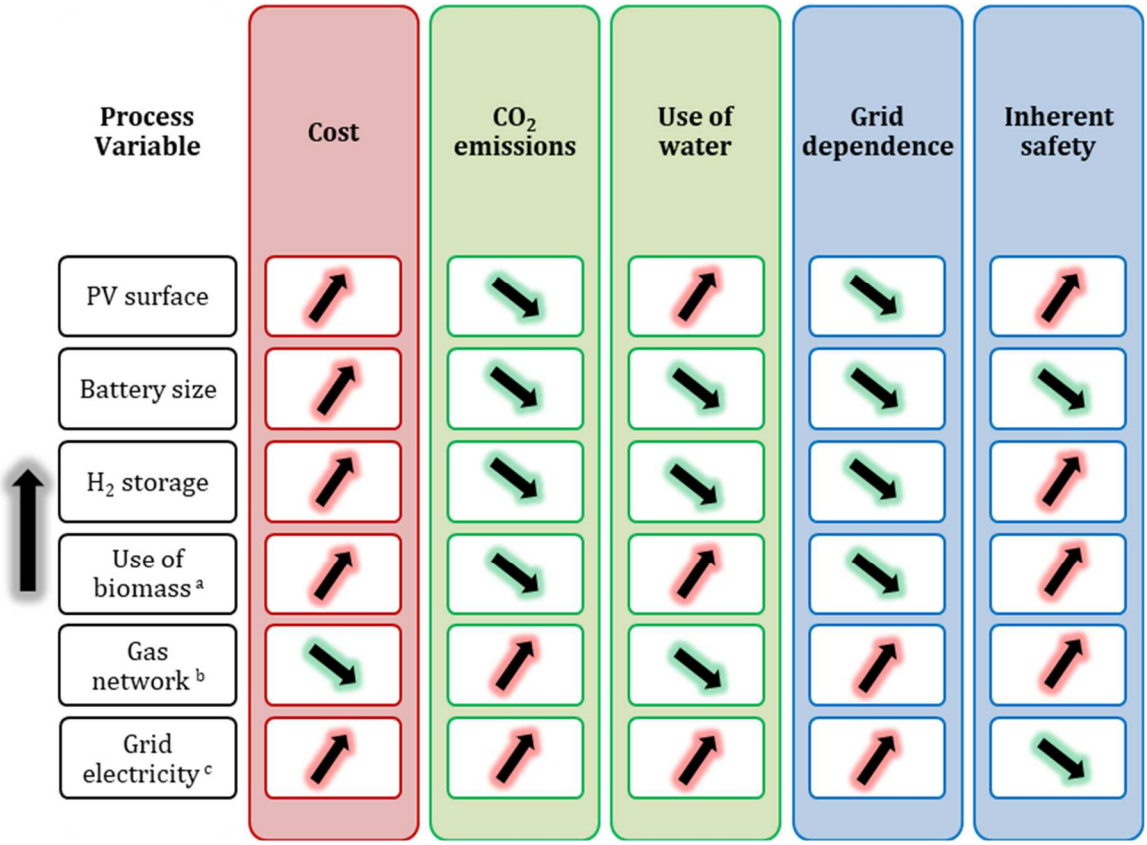

Figure 17. Impact of increasing the process variables on the sustainability indicators. (a) the use of biomass entails anaerobic digestion and reforming processes, (b) the gas network is used for steam methane reforming process, (c) grid is used for electrolysis of water.

Figure 17 presents the impact of the analyzed process variables on the sustainability indicators. It is worth bearing in mind that the performance of the indicators improves as their corresponding value decreases. In such a way, ascending and descending arrows represent negative and positive impacts, respectively. For instance, a larger surface of PV enables the reduction of CO_2 emissions and grid dependence as a higher amount of renewable-based

electricity is available. However, this also leads to a more expensive and potentially more hazardous energy system since bigger units for energy conversion and storage are needed. Besides, the performance of the water consumption indicator gets worse because the amount of water required for converting the surplus electricity into hydrogen also increases.

Regarding the alternatives for electricity storage, it is noted that both options enhance the indicators of the environmental dimension and promote the independence of the system for the energy supply. On the one hand, using energy storage technologies favors the exploitation of renewable-based electricity, since they enable to deal with the mismatch between electricity production and consumption. Thereby, CO_2 emissions and grid dependence indicators are improved because a lower amount of energy must be imported from the grid. On the other hand, the electrical battery does not require water for its operation, and the power-to-power system allows the recovery of water from the fuel cell to be reused in the electrolyzer. Consequently, they have a positive impact on the water consumption indicator. Additionally, the obtained results also indicate that the economic aspect is improved by reducing the size of the storage units, which evidences the competition among the sustainability indicators. Moreover, concerning the inherent safety of the system, results suggest reducing capacity of the pressurized tank as it represents the accumulation of a potentially hazardous material.

Otherwise, as observed in Figure 17, the impact of the technologies for obtaining hydrogen was also assessed. These alternatives include the use of biomass through the anaerobic digestion and the subsequent reforming process, the steam methane reforming of natural gas from the network, and the electrolysis of water by using electricity from the grid. In this regard, it is worth to note that no technology offers a solution able to simultaneously get the best performance of all the sustainability criteria. For instance, using biomass enables to reduce the CO_2 emissions and the dependence of the main grid, but at the cost of a higher investment, a more elevated water consumption, and riskier process conditions. Meanwhile, the gas network represents a better alternative from the economic point of view as the anaerobic digestion step is not required, and because of the low price of the natural gas. However, this pathway also leads to CO_2 emissions from fossil fuels, it corresponds to an option highly reliant on the main grid, and it entails the risk associated to the intense process conditions of the reforming reaction. In this respect, it is noted that the safety of the process can be improved by increasing the use of electricity from the grid for producing hydrogen. Nonetheless, in such a way, the performance of the other indicators becomes worse.

Conclusions

In this work a multi-objective optimization analysis for the design and operation of energy systems considering the sustainability dimensions was carried out. Moreover, two new

indicators, namely water consumption and inherent safety index, were included for the evaluation of the energy system design to enhance the environmental and social aspects. Then, these were added to a framework considering the total annualized cost, the CO_2 emissions, and the grid dependence to perform the multi-objective optimization. Altogether, four multi-objective optimization problems were formulated and solved for different combinations of the sustainability indicators. From multi-objective optimization results, the relationships among the objective functions were established, and a wide spread of plausible system configurations and operating conditions were obtained. Broadly, results reflect the compromise and the antagonistic behavior among the sustainability criteria. Thus, according to multi-objective optimization results, it was determined the competition between the total annualized cost and the CO_2 emissions and grid dependence objectives. In such a way, for a given surface of PV, the total annualized cost decreases as the performance in the emissions and self-sufficiency indicators gets worse. Also, outcomes indicate that the water consumption and the grid dependence are contradictory indicators. Likewise, the obtained results depict the competition between the inherent safety index with both the cost and emissions objectives. From this analysis, the following outcomes can be drawn:

- Depending on the objective function, the cost of energy range between 0.37 and 0.63 €/kWh and the CO_2 emissions vary between 10.6 and 68.5 $kgCO_2/MWh$.
- The best performance for the CO_2 emissions (10.6 $kgCO_2/MWh$) and grid dependence (20%) indicators entails to install the largest capacity of the storage units and the highest amount of equipment within the energy system. Consequently, this scenario leads to the energy system with the most elevated water consumption (70.2 m^3H_2O/GWh) and the most hazardous conditions.
- The water consumption can be reduced to around 28 m^3H_2O/GWh by producing the hydrogen by means of steam reforming of methane. Nevertheless, this also implies an energy system structure with the highest cost (0.63 €/kWh), CO_2 emissions (68.5 $kgCO_2/MWh$), and grid dependence (50%).
- The safest energy system conditions are obtained by producing the whole hydrogen through the water electrolysis route and by reducing the size of the pressurized tank as much as possible. Indeed, this configuration entails to install a PV area of 7500 m^2 and leads to a cost of energy of 0.54 €/kWh, an emission factor of 26 $kgCO_2/MWh$, and a water intensity of 57.5 m^3H_2O/GWh.

Otherwise, the set of Pareto solutions was explored and analyzed for identifying the changes in the design and operating conditions across the optimization results. Overall, these results could support the subsequent decision-making process since they depict the trade-off among the

sustainability dimensions, and the impact of any decision in terms of design and operation variables.

The proposed framework could be easily adapted and used for the design of energy systems in different context conditions, considering other criteria for evaluation, or including different technological units and energy forms. Moreover, as a perspective, the integration of the decision-maker preferences into the energy system design through a decision-aid making tool is envisaged. This would enable to classify the obtained Pareto sets and to select the most suitable alternative for its implementation.

Acknowledgment

This work was supported partly by the French PIA project « Lorraine Université d'Excellence », reference ANR-15-IDEX-04-LUE »

References

[1] International Energy Agency (IEA). Global Energy Review 2020. 2020.

[2] International Energy Agency (IEA). Global Energy & CO2 Status Report. 2019.

[3] International Renewable Energy Agency (IRENA). Global Energy transformation:A roadmap to 2050. Abu Dhabi: 2018.

[4] International Energy Agency (IEA). Status of Power System Transformation 2019: Power System Flexibility. 2019.

[5] REN21. Renewables 2019 Global Status Report. Paris: 2019.

[6] Liu P, Georgiadis MC, Pistikopoulos EN. An energy systems engineering approach for the design and operation of microgrids in residential applications. Chem Eng Res Des 2013;91:2054–69. https://doi.org/10.1016/j.cherd.2013.08.016.

[7] Mavromatidis G, Orehounig K, Bollinger LA, Hohmann M, Marquant JF, Miglani S, et al. Ten questions concerning modeling of distributed multi-energy systems. Build Environ 2019;165:106372. https://doi.org/10.1016/j.buildenv.2019.106372.

[8] Dimian AC, Bildea CS, Kiss AA. Integrated Design and Simulation of Chemical Processes. Second edi. Amsterdam: Elsevier B.V; 2014.

[9] Smith R. Chemical Process Design and Integration. John Wiley & Sons, Ltd; 2005.

[10] Ruiz-mercado G, Cabezas H. Sustainability in the Design, Synthesis and Analysis of Chemical Engineering Processes. Elsevier - Butterworth-Heinemann; 2016.

[11] Bakshi BR, Fiksel J. The quest for sustainability: Challenges for process systems engineering. AIChE J 2003;49:1350–8. https://doi.org/10.1002/aic.690490602.

[12] Rong A, Lahdelma R. Role of polygeneration in sustainable energy system development

challenges and opportunities from optimization viewpoints. Renew Sustain Energy Rev 2016;53:363–72. https://doi.org/10.1016/j.rser.2015.08.060.

[13] Alanne K, Saari A. Distributed energy generation and sustainable development. Renew Sustain Energy Rev 2006;10:539–58. https://doi.org/10.1016/j.rser.2004.11.004.

[14] Adil AM, Ko Y. Socio-technical evolution of Decentralized Energy Systems: A critical review and implications for urban planning and policy. Renew Sustain Energy Rev 2016;57:1025–37. https://doi.org/10.1016/j.rser.2015.12.079.

[15] Gabrielli P, Gazzani M, Martelli E, Mazzotti M. Optimal design of multi-energy systems with seasonal storage. Appl Energy 2018;219:408–24. https://doi.org/10.1016/j.apenergy.2017.07.142.

[16] Gabrielli P, Fürer F, Mavromatidis G, Mazzotti M. Robust and optimal design of multi-energy systems with seasonal storage through uncertainty analysis. Appl Energy 2019;238:1192–210. https://doi.org/10.1016/j.apenergy.2019.01.064.

[17] Jing R, Wang M, Liang H, Wang X, Li N, Shah N, et al. Multi-objective optimization of a neighborhood-level urban energy network: Considering Game-theory inspired multi-benefit allocation constraints. Appl Energy 2018;231:534–48. https://doi.org/10.1016/j.apenergy.2018.09.151.

[18] Falke T, Krengel S, Meinerzhagen AK, Schnettler A. Multi-objective optimization and simulation model for the design of distributed energy systems. Appl Energy 2016;184:1508–16. https://doi.org/10.1016/j.apenergy.2016.03.044.

[19] Ren H, Zhou W, Nakagami K, Gao W, Wu Q. Multi-objective optimization for the operation of distributed energy systems considering economic and environmental aspects. Appl Energy 2010;87:3642–51. https://doi.org/10.1016/j.apenergy.2010.06.013.

[20] Di Somma M, Yan B, Bianco N, Graditi G, Luh PB, Mongibello L, et al. Multi-objective design optimization of distributed energy systems through cost and exergy assessments. Appl Energy 2017;204:1299–316. https://doi.org/10.1016/j.egypro.2017.03.706.

[21] Dorotić H, Pukšec T, Duić N. Multi-objective optimization of district heating and cooling systems for a one-year time horizon. Energy 2019;169:319–28. https://doi.org/10.1016/j.energy.2018.11.149.

[22] Dorotić H, Pukšec T, Duić N. Economical, environmental and exergetic multi-objective optimization of district heating systems on hourly level for a whole year. Appl Energy 2019;251:113394. https://doi.org/10.1016/j.apenergy.2019.113394.

[23] Dufo-López R, Bernal-Agustín JL. Multi-objective design of PV-wind-diesel-hydrogen-battery systems. Renew Energy 2008;33:2559–72. https://doi.org/10.1016/j.renene.2008.02.027.

[24] Cedillos Alvarado D, Acha S, Shah N, Markides CN. A Technology Selection and Operation (TSO) optimisation model for distributed energy systems: Mathematical formulation and case study. Appl Energy 2016;180:491–503. https://doi.org/10.1016/j.apenergy.2016.08.013.

[25] Mayer MJ, Szilágyi A, Gróf G. Environmental and economic multi-objective optimization of a household level hybrid renewable energy system by genetic algorithm. Appl Energy 2020;269:115058. https://doi.org/10.1016/j.apenergy.2020.115058.

[26] Hou J, Wang J, Zhou Y, Lu X. Distributed energy systems: Multi-objective optimization and evaluation under different operational strategies. J Clean Prod 2021;280:124050. https://doi.org/10.1016/j.jclepro.2020.124050.

[27] Karmellos M, Mavrotas G. Multi-objective optimization and comparison framework for the design of Distributed Energy Systems. Energy Convers Manag 2019;180:473–95. https://doi.org/10.1016/j.enconman.2018.10.083.

[28] Yan J, Broesicke OA, Tong X, Wang D, Li D, Crittenden JC. Multidisciplinary design optimization of distributed energy generation systems: The trade-offs between life cycle environmental and economic impacts. Appl Energy 2020;284:116197. https://doi.org/10.1016/j.apenergy.2020.116197.

[29] Weinand JM, Scheller F, McKenna R. Reviewing energy system modelling of decentralized energy autonomy. Energy 2020;203:117817. https://doi.org/10.1016/j.energy.2020.117817.

[30] Campos-Guzmán V, García-Cáscales MS, Espinosa N, Urbina A. Life Cycle Analysis with Multi-Criteria Decision Making: A review of approaches for the sustainability evaluation of renewable energy technologies. Renew Sustain Energy Rev 2019;104:343–66. https://doi.org/10.1016/j.rser.2019.01.031.

[31] Azapagic A, Stamford L, Youds L, Barteczko-Hibbert C. Towards sustainable production and consumption: A novel DEcision-Support Framework IntegRating Economic, Environmental and Social Sustainability (DESIRES). Comput Chem Eng 2016;91:93–103. https://doi.org/10.1016/j.compchemeng.2016.03.017.

[32] United Nations. Sustainable Development Goals. Goal 6 Ensure Access to Water Sanit All 2020. https://www.un.org/sustainabledevelopment/water-and-sanitation/ (accessed May 16, 2020).

[33] Evans A, Strezov V, Evans TJ. Assessment of sustainability indicators for renewable energy technologies. Renew Sustain Energy Rev 2009;13:1082–8. https://doi.org/10.1016/j.rser.2008.03.008.

[34] Ruiz-Mercado GJ, Smith RL, Gonzalez MA. Sustainability indicators for chemical processes: I. Taxonomy. Ind Eng Chem Res 2012;51:2309–28. https://doi.org/10.1021/ie102116e.

[35] Shaaban M, Scheffran J. Selection of sustainable development indicators for the assessment of electricity production in Egypt. Sustain Energy Technol Assessments 2017;22:65–73. https://doi.org/10.1016/j.seta.2017.07.003.

[36] Moslehi S, Arababadi R. Sustainability Assessment of Complex Energy Systems Using Life Cycle Approach-Case Study: Arizona State University Tempe Campus. Procedia Eng 2016;145:1096–103. https://doi.org/10.1016/j.proeng.2016.04.142.

[37] Abu-Rayash A, Dincer I. Sustainability assessment of energy systems: A novel integrated model. J Clean Prod 2019;212:1098–116. https://doi.org/10.1016/j.jclepro.2018.12.090.

[38] International Atomic Energy Agency (IAEA), United Nations Department of Economic and Social Affairs, International Energy Agency (IEA), EUROSTAT, European Environment Agency. Energy Indicators for Sustainable Development : Guidelines and Methodologies. 2005.

[39] United Nations. Sustainable Development Goals. Goal 7 Afford Clean Energy 2020. https://www.un.org/sustainabledevelopment/energy/ (accessed May 12, 2020).

[40] Santoyo-Castelazo E, Azapagic A. Sustainability assessment of energy systems: Integrating environmental, economic and social aspects. J Clean Prod 2014;80:119–38. https://doi.org/10.1016/j.jclepro.2014.05.061.

[41] Stamford L, Azapagic A. Sustainability indicators for the assessment of nuclear power. Energy 2011;36:6037–57. https://doi.org/10.1016/j.energy.2011.08.011.

[42] Park S, Xu S, Rogers W, Pasman H, El-Halwagi MM. Incorporating inherent safety during the conceptual process design stage: A literature review. J Loss Prev Process Ind 2020;63:104040. https://doi.org/10.1016/j.jlp.2019.104040.

[43] Roy N, Eljack F, Jiménez-Gutiérrez A, Zhang B, Thiruvenkataswamy P, El-Halwagi M, et al. A review of safety indices for process design. Curr Opin Chem Eng 2016;14:42–8. https://doi.org/10.1016/j.coche.2016.07.001.

[44] Fonseca JD, Commenge J-M, Camargo M, Falk L, Gil ID. Multi-criteria optimization for the design and operation of distributed energy systems considering sustainability dimensions. Energy 2021;214. https://doi.org/10.1016/j.energy.2020.118989.

[45] Association française pour l'hydrogene et les piles à combustible (AFHYPAC). Production D'Hydrogene Par Electrolyse De L'Eau. vol. Fiche 3.2. 2019.

[46] Angelonidi E, Smith SR. A comparison of wet and dry anaerobic digestion processes for the treatment of municipal solid waste and food waste. Water Environ J 2015;29:549–57. https://doi.org/10.1111/wej.12130.

[47] Athar M, Shariff AM, Buang A. A review of inherent assessment for sustainable process design. J Clean Prod 2019;233:242–63. https://doi.org/10.1016/j.jclepro.2019.06.060.

[48] Song D, Yoon ES, Jang N. A framework and method for the assessment of inherent safety to enhance sustainability in conceptual chemical process design. J Loss Prev Process Ind 2018;54:10–7. https://doi.org/10.1016/j.jlp.2018.02.006.

[49] Rahman M, Heikkilä AM, Hurme M. Comparison of inherent safety indices in process concept evaluation. J Loss Prev Process Ind 2005;18:327–34. https://doi.org/10.1016/j.jlp.2005.06.015.

[50] Jafari MJ, Mohammadi H, Reniers G, Pouyakian M, Nourai F, Torabi SA, et al. Exploring inherent process safety indicators and approaches for their estimation: A systematic review. J Loss Prev Process Ind 2018;52:66–80. https://doi.org/10.1016/j.jlp.2018.01.013.

[51] Heikkilä AM. Inherent safety in process plant design. An index-based approach. Helsinki University of Technology, 1999.

[52] Kletz T, Amyotte P. Process plants: A handbook for inherently safer design. Second. Boca Raton: CRC Press; 2010. https://doi.org/10.1201/9781439804568.

[53] Li X, Zanwar A, Jayswal A, Lou HH, Huang Y. Incorporating exergy analysis and inherent safety analysis for sustainability assessment of biofuels. vol. 50. 2011. https://doi.org/10.1021/ie101660q.

[54] Laurence D. Quantifying inherent safety of chemical process routes. Loughborough University of Technology, 1996.

[55] Gangadharan P, Singh R, Cheng F, Lou HH. Novel Methodology for Inherent Safety Assessment in the Process Design Stage. Ind Eng Chem Res 2013;52:5921–33. https://doi.org/10.1021/ie303163y.

[56] (ADEME) Agence de l'Environnement et de la Maîtrise de l'Energie. MODECOM 2017 Campagne nationale de caractérisation des déchets ménagers et assimilés. Angers: 2019.

[57] (ADEME) Agence de l'Environnement et de la Maîtrise de l'Energie. Déchets Chiffres-clés. Angers: 2018.

[58] Pandu Rangaiah G. Multi-objective Optimization: Techniques and Applications in Chemical Engineering. Singapore: World Scientific Publishing; 2009.

https://doi.org/10.1007/978-1-84800-382-8_2.

[59] Diwekar U. Introduction to Applied Optimization. Second edi. Springer; 2008. https://doi.org/10.1007/978-0-387-73669-3.

[60] Coello Coello CA, Lamont GB, Veldhuizen DA Van, Goldberg DE, Koza JR. Evolutionary Algorithms for Solving Multi-Objective Problems. Second edi. Springer; 2007. https://doi.org/10.1007/978-0-387-36797-2.

[61] Pandu Rangaiah G, Bonilla-Petriciolet A. Multi-Objective Optimization in Chemical Engineering: Developments and Applications. John Wiley & Sons, Ltd; 2013. https://doi.org/10.6028/jres.090.045.

[62] Cui Y, Geng Z, Zhu Q, Han Y. Review: Multi-objective optimization methods and application in energy saving. Energy 2017;125:681–704. https://doi.org/10.1016/j.energy.2017.02.174.

Graphical Abstract